Journal of Cleaner Production 348 (2022) 131285

Contents lists available at ScienceDirect

Journal of Cleaner Production

journal homepage: www.elsevier.com/locate/jclepro

Predictive modeling of compressive strength of sustainable rice husk ash concrete: Ensemble learner optimization and comparison

Bawar Iftikhar [a,b], Sophia C. Alih [c], Mohammadreza Vafaei [a], Mohamed Abdelghany Elkotb [d,e], Meshal Shutaywi [f], Muhammad Faisal Javed [b], Wejdan Deebani [f], M. Ijaz Khan [g,h,*], Fahid Aslam [i]

[a] School of Civil Engineering, Universiti Teknologi Malaysia, 81310, Johor Bahru, Johor, Malaysia
[b] Department of Civil Engineering, COMSATS University Islamabad, Abbottabad Campus, 22060, Pakistan
[c] Institute of Noise and Vibration, School of Civil Engineering, Universiti Teknologi Malaysia, 81310, Johor Bahru, Johor, Malaysia
[d] Mechanical Engineering Department, College of Engineering, King Khalid University, Abha, 61421, Saudi Arabia
[e] Mechanical Engineering Department, Faculty of Engineering, Kafrelsheikh University, 33516, Egypt
[f] King Abdulaziz University, College of Science & Arts, Department of Mathematics, Rabigh, Saudi Arabia
[g] Department of Mechanics and Engineering Science, Peking University, Beijing, 100871, People's Republic of China
[h] Department of Mathematics and Statistics, Riphah International University I-14, Islamabad, 44000, Pakistan
[i] Department of Civil Engineering, College of Engineering in Al-Kharj, Prince Sattam Bin Abdulaziz University, Al-Kharj, 11942, Saudi Arabia

ARTICLE INFO

Handling Editor: Prof. Jiri Jaromir Klemeš

Keywords:
Machine learning
Rice husk ash concrete
Modeling
Random forest
Gene expression programming

ABSTRACT

One of the largest sources of greenhouse gas (GHG) emissions is the construction concrete industry which has alone 50% of the world's emissions. One possible remedy to mitigate the effect of environmental issues is the use of waste and recycled material in concrete. Today, immense agricultural waste is being used as a substitute for cement in the production of sustainable concrete. Therefore, this study is aimed to predict and develop an empirical formula of the compressive strength of rice husk ash (RHA) concrete using machine learning algorithms. Methods employed in this study includes gene expression programming (GEP) and Random Forest Regression (RFR). A reliable database of 192 data points was employed for developing the models. Most influential variables including age, cement, rice husk ash, water, super plasticizer, and aggregate were employed as input parameters in the development of RHA-based concrete models. Evaluation of models was performed using different statistical parameters. These statistical measures include mean absolute error (MAE), coefficient of determination (R^2), performance index (ρ), root man square error (RMSE), relative squared error (RSE) and relative root mean square (RRMSE). The GEP model outperforms the RFR ensemble model in terms of robustness, with a greater correlation of $R^2 = 0.96$ compared to RFR's $R^2 = 0.91$. Ensemble modeling showed an enhancement of 1.62 percent for RFR compressive strength model when compared with individual RFR compressive strength model as illustrated by statistical parameters. Moreover, GEP model shows an enhancement of 37.33 percent in average error with an average error 2.35 MPa as compared to RFR model with average error of about 3.75 MPa. Cross validation was used as external check to avoid overfitting issues of the models and confirm the generalized model output. Parametric analysis was performed to determine the impact of the input parameters on the output. Cement and age were shown to have a substantial impact on the compressive strength of RHA concrete using sensitivity analysis.

1. Introduction

Increasing greenhouse gas (GHG) emissions have led to the melting of polar ice caps in the Arctic and Antarctic regions. This has led to serious environmental issues on the planet earth (Eijgelaar et al., 2010). Construction concrete industry is one of the largest sources of GHG emissions with alone 50% of the world's emissions (Arrigoni et al., 2020). The increasing demand for concrete is still an upsurge in the construction industry. Portland cement (PC) is one of the most important concrete parameters that contribute significantly to GHG (Rehan and Nehdi, 2005). Production of cement contributes around 7% of global

* Corresponding author. Department of Mechanics and Engineering Science, Peking University, Beijing, 100871, People's Republic of China.
E-mail address: mikhan@math.qau.edu.pk (M.I. Khan).

https://doi.org/10.1016/j.jclepro.2022.131285
Received 25 December 2021; Received in revised form 4 March 2022; Accepted 7 March 2022
Available online 15 March 2022

CO_2 emissions to the atmosphere. Moreover, by the calcination of calcium oxide, concrete production generates 50% of CO_2 emissions

Notations

ANN	artificial neural network
ET	expression tree
GEP	genetic engineering programming
GHG	greenhouse gas
RHA	rice husk ash
DT	decision tree
SCMs	supplementary cementations materials
KFCV	K-Fold cross validation
ML:	machine learning
MSE	mean squared error
PA	parametric analysis
PC	Portland cement
R^2	coefficient of determination
RFR	random forest regressions
RHA	rice husk ash
RMSE	root mean squared error
SA	sensitivity analysis
SVM	support vector machine

Fig. 1. Manufacturing of sustainable and ecofriendly concrete.

(Benhelal et al., 2013). The annual consumption of cement is around 4000 million tons and is expected to be increased by 2060 by around 6000 million tons (Shahmansouri et al., 2020). These GHG emissions have had a key role in climate change. Recent years have seen an increase in the number of detailed research on the various causes of climate change (both natural and manmade), their consequences on living circumstances, and viable strategies of adaptation and mitigation (Tin Lee et al., 2016; Giorgio et al., 2009). Due to the energy-intensive and emission-intensive manufacturing process of ordinary Portland cement (OPC), blended cement manufacture requires the use of a variety of alternative cementitious ingredients (Mikulčić et al., 2016). The use of industrial by-products as supplemental cementitious materials (SCMs)

Fig. 2. Effect on concrete properties by using waste materials.

is one such strategy that has resulted in a large decrease in the use of traditional Portland cement while also removing the hazards associated with the disposal of waste materials from diverse industries (Rahla et al., 2019). In 2004, the use of industrial by-products as raw materials in blended cement production resulted in a savings of approximately 14 million tonnes of traditional raw materials, or approximately 6.5 percent of the natural raw materials required (Schorcht et al., 2013). Thus, the most effective strategy to lower the carbon footprint of the building sector is to substitute acceptable alternative cementitious materials for Portland cement clinker (Supino et al., 2016). These figures show that viable alternatives are required to meet high concrete demands with lower energy usage and emissions of CO_2 (Buchanan and Levine, 1999; Liu et al., 2021). The use of waste and recycled material in concrete is one of the feasible remedies to mitigate the effect of environmental issues. This will not only meet the growing demand for concrete but also decreases the immediate risk to the community (Tam and Tam, 2006). The use of waste materials including supplementary cementations materials (SCMs) has been a keen focus of many researchers in the construction industry (Tang et al., 2020; hai He et al., 2021a). The preparation of ecofriendly concrete has been of great importance (Shi et al., 2021). The enormous agriculture waste like rick husk ash (RHA), palm oil fuel ash (POFA), sugarcane bagasse ash (SBA), olive oil ash (OOA), and industrial waste such as fly ash (FA), silica fume (SF) are used today as a part of cement replacement in the manufacturing of sustainable concrete as illustrated in Fig. 1 (Aprianti S, 2017). Dumping this agricultural and industrial waste product in open land poses a serious environmental hazard by contaminating air and water systems (Ihedioha et al., 2017). Furthermore, around 110 million tonnes of rice husk (almost 20% of 550 million tonnes of rice) and 16–22 million tonnes of RHA are produced globally (* Energy Technology). Using the waste materials in the concrete can improve both concrete's durability and strength due to the action of pozzolanic nature (hai He et al., 2021b). This reduces industry demand for cement, minimizing the cost of manufacturing concrete and decreasing the undesirable effects of CO_2 emissions into the manufacturing of cement (Mikulčić et al., 2016).

Concrete is commonly used as a construction material all over the world, because of its many advantages, including economic

Table 1
Summarize machine learning algorithm by researchers.

S. No	Machine learning method	Abbreviation	Data set	Prediction property	Year	Waste materials	References
1.	Gene expression programming	GEP	298	Compressive Strength	2021	FA	Khan et al. (2021a)
2.	Conventional Artificial Neural Network	C-ANN	220	Compressive Strength	2020	Foamed concrete	Van Dao et al. (2020)
3.	Gene expression programming	GEP	351	Compressive Strength	2020	GGBFS	Shahmansouri et al. (2020)
4.	Gene expression programming	GEP	168	Tensile Strength	2012	Normal concrete	Severcan (2012)
5.	Gene expression programming	GEP	160	Post fire behavior	2020	GGBFS	Fakhrian et al. (2020)
6.	Artificial Neural Network Multi Linear Regression	ANN and MLR	1288	Compressive strength	2015	Clinker mortar	Beyciołlu et al. (2015)
7.	Artificial Neural Network	ANN	264	Thermal properties	2019	Silica fume	Fidan et al. (2019)
8.	Support Vector Machine	SVM	15	Compressive strength	2021	Normal concrete	Lv et al. (2021)
9.	Support Vector Machine Random forest AdaBoost	SVM RF AB	288	Compressive Strength	2017	Blast furnance slag and waste tire rubber powder	Ozcan et al. (2017)
10.	Support Vector Machine Adaptive-Network-based Fuzzy Inference System	SVM-ANFIS	120	Deflection	2020	RC beam	Bai et al. (2020)
11.	Ensemble models	RT, RF, GBRT, ensemble GBRT	126	Unconfined compressive strength	2019	Cemented Paste Backfill	Lu et al. (2019b)
12.	Artificial neuron network	ANN	169	Compressive strength	2016	FA GGBFS SF RHA	Asteris et al. (2016)
13.	Artificial neuron network	ANN	205	Compressive strength	2019	FA GGBFS SF RHA	Asteris and Kolovos (2019)
14.	Artificial neuron network	ANN	69	Compressive strength	2017	FA	Abu Yaman et al. (2017)
15.	Artificial neuron network	ANN	114	Compressive strength	2017	FA	Belalia Douma et al. (2017)
16.	Artificial neuron network	ANN	80	Compressive strength	2011	FA	Siddique et al. (2011)
17.	Artificial neuron network	ANN	300	Compressive strength	2009	FA	Prasad et al. (2009)
18.	Adaptive neuro fuzzy inference system	ANFIS	55	Compressive strength	2018	–	Vakhshouri and Nejadi (2018)
19.	Support vector machine	SVM	–	Compressive strength	2020	FA	Azimi-Pour et al. (2020)
20.	Random forest	RF	131	Compressive strength	2019	FA GGBFS SF	Zhang et al. (2019)
21.	Multivariate	MV	21	Compressive strength	2020	Crumb rubber with SF	Bušić et al. (2020)
22.	Biogeographical-based programming	BBP	413	Elastic modulus		SF FA SLAG	Golafshani and Ashour (2016)
23.	Intelligent rule-based enhanced multiclass support vector machine and fuzzy rules	IREMSVM-FR with RSM	114	Compressive strength	2019	FA	Selvaraj and Sivaraman (2019)
24.	Support vector machine	SVM	115	Slump test L-box test V-funnel test Compressive strength	2020	FA	Saha et al. (2020)
25.	Multivariate adaptive regression spline	M5 MARS	114	Compressive strength Slump test L-box test V-funnel test	2018	FA	Kaveh et al. (2018)
26.	Random Kitchen Sink Algorithm	RKSA	40	V-funnel test J-ring test Slump test Compressive strength	2018	FA	Sathyan et al. (2018)
27.	Data Envelopment Analysis	DEA	114	Compressive strength Slump test L-box test V-funnel test	2021	FA	Balf et al. (2020)
28.	Adaptive neuro fuzzy inference system	ANFIS with ANN	7	Compressive strength	2020	POFA	Al-Mughanam et al. (2020)
29.	Gene expression programming	GEP	277	Axial capacity	2020	–	Javed et al. (2020)
30.			357	Compressive strength	2020	–	Aslam et al. (2020)
31.	Random forest and gene expression programming	RF and GEP	357	Compressive strength	2020	–	Farooq et al. (2020)
32.	Individual with ensemble modeling	ANN, bagging and boosting	1030	Compressive strength	2021	FA GGBFS	Farooq et al. (2021)

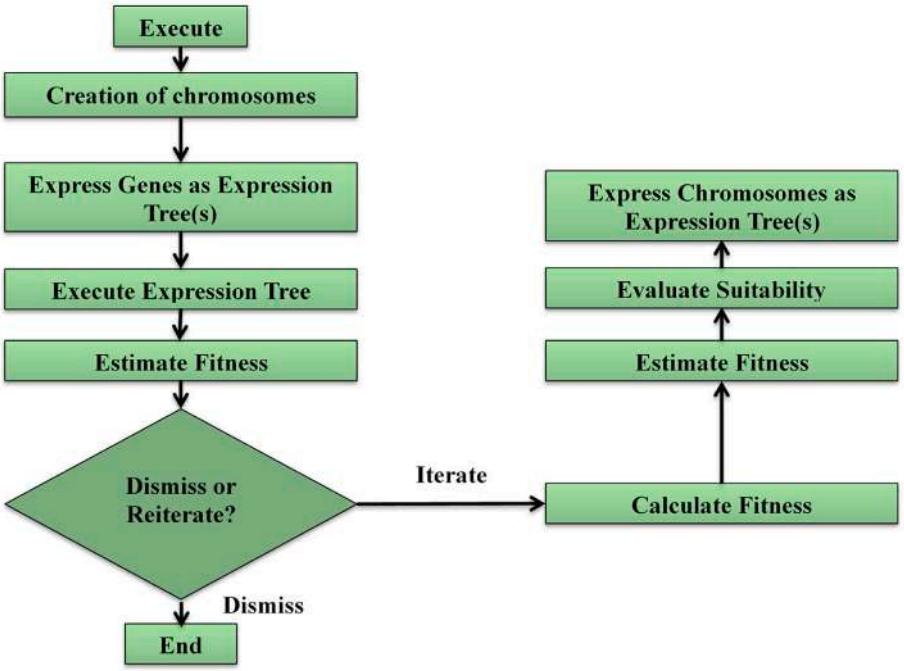

Fig. 3. Flow diagram of the GEP algorithm.

performance, modularity integrity, and durability (Cao et al., 2015). The compressive strength of concrete is considered the most important property because it directly affects the durability of constructed objects (Saloma et al., 2015). Concrete contains gravel, sand, cement, along with that it also contains supplementary raw material and admixtures. The combination of these parameters altogether in the concrete mix design is distributed randomly (Xiao, 2018). The use of RHA as SCM will affect various factors such as compressive loading ability, including the waste composition, particle size, and the aggregate water-to-cement ratio (Paris et al., 2016). Moreover, their use in concrete increases the compressive strength, reduces CO_2 emission, and increases the tensile strength as shown in Fig. 2. Thus, in such a complex matrix, it is very difficult to estimate the compression strength of the concrete. Physical checks are conducted to measure the compressive capacity of the concrete (Napoli and Realfonzo, 2020). Generally, specimens of concrete in cubic and cylindrical form are developed to check the strength of mortar and concrete. However, it is less effective, less economical, and needs a great deal of time in laboratory and field testing to measure the desire strength. Thus, empirical and machine learning (ML) regression methods are employed to test the ability of concrete (Chou et al., 2014; Ben Chaabene et al., 2020). The estimation of the compressive load capacity of concrete is just one application of the machine learning regression function. Moreover, it can also be used for clustering and classification of samples.

2. Literature with research

Different computational and numerical techniques have been performed in various fields to predict the desired outcomes (Zha et al., 2021; Zhao et al., 2021a; Chu et al., 2022; Lu et al., 2019a; Liu et al., 2020; He et al., 2022). Similarly, Tie et al. (Zhao et al., 2021b) employed ANN analysis for heat and entropy generation in flow of non-Newtonian fluid between two rotating disks. Khan et al. (2021a) predicted the mechanical properties of geopolymer concrete by using ensemble and individual algorithms. The author reveals that GEP give empirical equation which can predict the FA based GP concrete. However, ensemble model give better accuracy as compared to GEP with coefficient of determination R^2 of 0.972 as compared to individual algorithms. Dao et al. (Van Dao et al., 2020) used conventional artificial neural network (C-ANN) technique on foamed concrete to predict its compressive strength. The study demonstrates that ANN is a highly efficient for predicting the compressive strength of foamed concrete with a maximum coefficient value of 0.976 for the training set and 0.972 for the testing set. Shahmansouri et al. (2020) developed a numerical model using GEP that can predict the compressive strength of geopolymer concrete (GPC). The author obtained best model for training and validation set with R^2 of 0.91 and 0.94 respectively. The results for most of the models were satisfactory and similar to that of the experiments. Moreover, Severcan et al. (Severcan, 2012) proposed a formulation to predict the tensile strength of cylinder through GEP. The author reported that input parameters play a vital role with water to binder ratio has been most effective in strength prediction. Fakhrian et al. (2020) predicted the post fire behavior of geopolymer mortar through GEP technique which contained recycle concrete aggregate. The training and validation phases with a determination coefficient between 0.95 and 0.99 showed that the results predicted in the proposed models were properly consistent with the testing results. Beycioglu et al. (Beycioğlu et al., 2015) assessed the compressive strengths of clinker mortar with the ANN and Multiple Linear Regressions (MLR) model. ANN has shown a satisfactory relationship to experimental results and suggests an alternative approach for evaluating clinker mortar compression strength using affiliated inputs. In addition, MLR model has shown poor predictability as compared to ANN model. Fidan et al. (2019) developed an artificial network neural ANN model to predict concrete thermal properties. The author concluded that ANN model shows overall best performance for thermal conductivity, thermal diffusivity and specific heat with R^2 of 0.996, 0.983, and 0.995 respectively. Farooq et al. (2020) used an ensemble random forest (RF) and gene expression program (GEP) algorithm for the prediction of high strength concrete (HSC). The RF and GEP models are comparable to individual algorithms. RF nevertheless outbursts and gives $R^2 = 0.96$ with lesser errors as compared to DT and ANN. Similiarly, ahmad et al. (Ahmad et al., 2021) studied and predicted the response of FA based concrete using various algorithms. The algorithms used show a significant impact on the quality of the model with better accuracy. A better outcome with $R^2 = 0.911$ is achieved with the ensemble model in contrast to the individual model

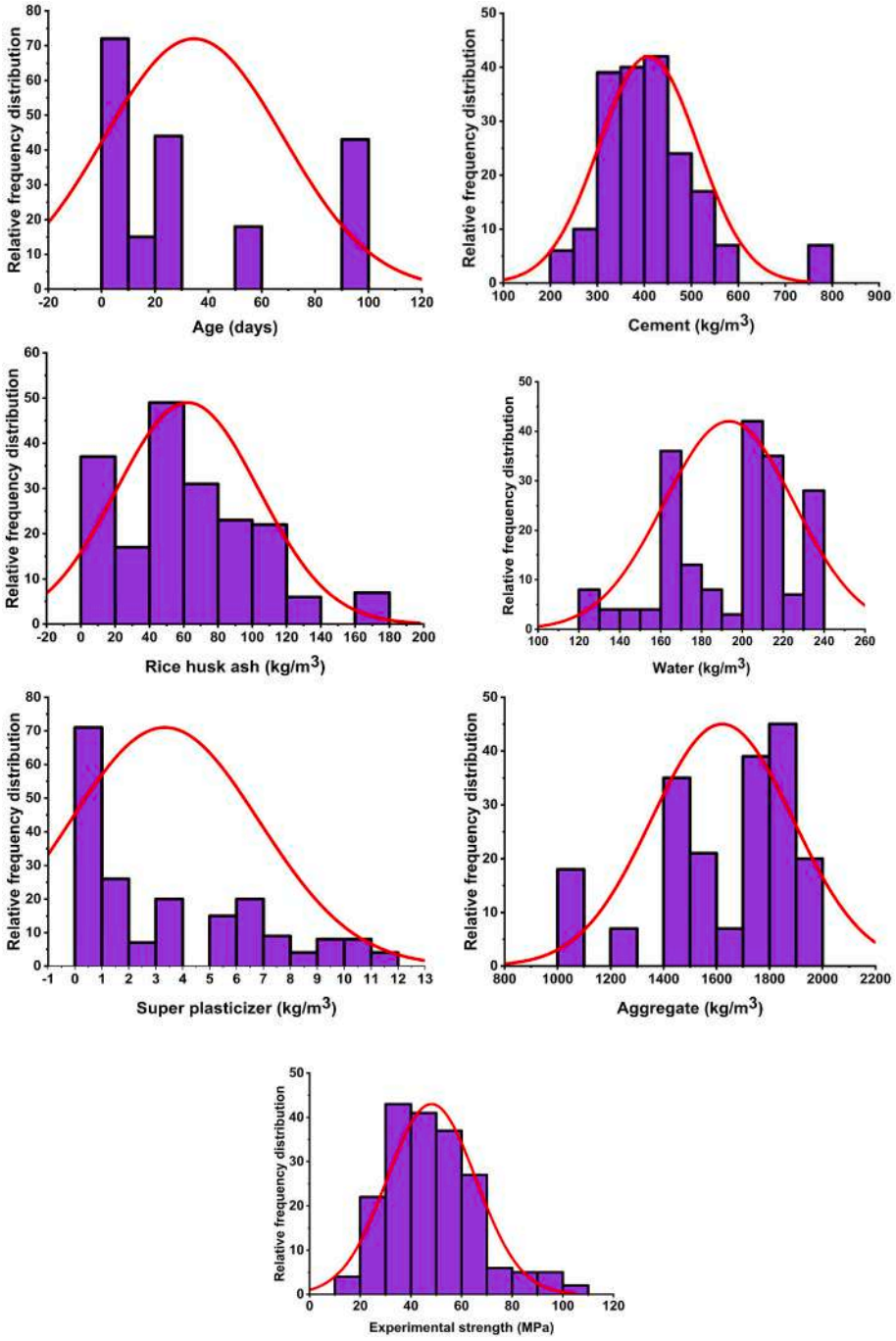

Fig. 4. Frequency distribution of data used in making model.

where $R^2 = 0.812$ is achieved. Zhiqiang et al. (Lv et al., 2021) established the acoustic emission (AE) series multifractal damage analysis and offers an SVM model in which concrete strength of concrete is predicted by AE parameters. The R^2 correlation coefficients were found to be equal to about 1. The concrete strength obtained from the proposed SVM model is indicated to be in good response with the experimental value. Ozcan et al. (2017) developed machine learning models to estimate the compressive strength of cement with blast furnace slag (BFS) and waste tire rubber powder (WTRP). The experiments with the dataset produced noticeable good outputs with higher determination coefficients. Moreover, ada Boost algorithm outburst among the other learning algorithms. Bai et al. (2020) addressed an essential technical problem in construction and civil engineering, namely the prediction of the deflection of reinforced concrete beams. It was shown that the SVM-ANFIS ensemble models can predict with high precision for the deflection of reinforced concrete beams. Khoa et al. (Nguyen et al., 2020) predicted the compressive strength of fly ash based geopolymer concrete using DNN and ResNet techniques. Statistical parameters indicated strong correlation of the anticipated results with the experimental values. Similarly, machine learning algorithms was utilized to predict the compressive and split tensile strength of concrete using RHA as cement replacement and glass fiber as an additive (Haque et al., 2021). It was found that predicted results values were close to that of experimental results. Mustafa (Saridemir, 2010) employed GEP to predict the strength of concrete containing RHA at different ages and found adequate results. Lu et al. (2019b) employed the ensemble learning method to improve the cemented paste backfill of unconfined compressive strength (UCS). The R values obtained by ensemble

Table 2
Descriptive statistics of variables used in modeling aspect.

Statistical details	Age	Cement	Rice husk ash	Water	Super plasticizer	Aggregate
Mean	34.57	409.02	62.33	193.54	3.34	1621.51
Standard Error	2.42	7.61	3.00	2.30	0.25	19.32
Median	28.00	400.00	57.00	203.00	1.85	1725.00
Mode	28.00	400.00	0.00	203.00	0.00	1725.00
Standard Deviation	33.52	105.47	41.55	31.93	3.52	267.77
Sample Variance	1123.61	11124.88	1726.77	1019.71	12.37	71702.44
Kurtosis	−1.02	3.66	0.07	−0.74	−0.82	−0.27
Skewness	0.75	1.55	0.44	−0.42	0.69	−0.74
Range	89.00	534.00	171.00	118.00	11.25	930.00
Minimum	1.00	249.00	0.00	120.00	0.00	1040.00
Maximum	90.00	783.00	171.00	238.00	11.25	1970.00
Sum	6638.00	78531.00	11967.10	37158.91	640.35	311330.00
Count	192.00	192.00	192.00	192.00	192.00	192.00

Table 3
Variable correlations.

	Age	Cement	RHA	Water	Super plasticizer	Aggregate	Strength
Age	1						
Cement	−0.10565	1					
RHA	−0.03263	−0.21938	1				
Water	0.010909	0.083087	0.135647	1			
Super plasticizer	-3E-05	0.252929	−0.02092	0.267961	1		
Aggregate	−0.06306	−0.23787	−0.13868	−0.54908	−0.20521	1	
Strength	0.494869	0.370099	−0.02291	−0.24353	0.301277	0.146561	1

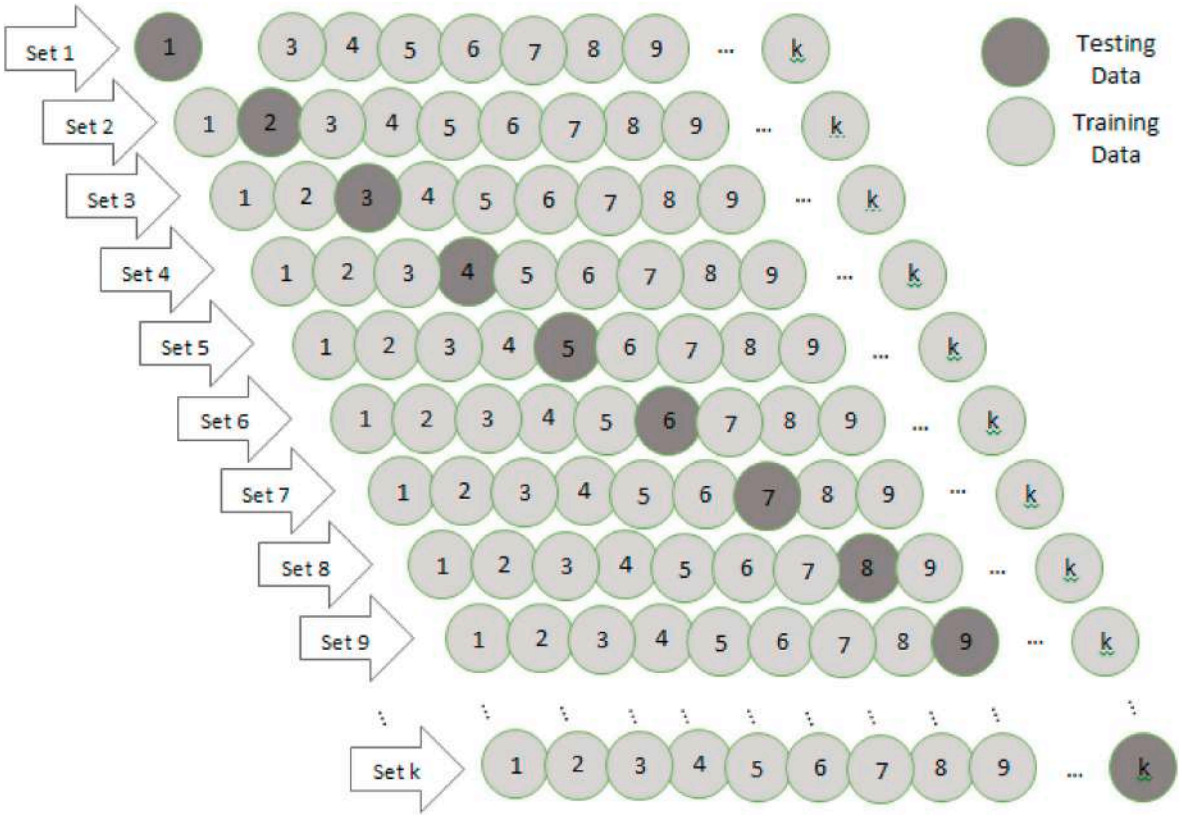

Fig. 5. K-Fold cross validation with testing and training set.

regressor were much accurate as compared to other model methods. Moreover the prediction property by different researcher is also summarized in Table 1.

3. Machine learning modeling approach

Machine learning methods have been used by various researchers to estimate and understand the material's properties and behavior of concrete. In this study, the compressive strength of RHA based concrete

Table 4
Statistical metrics suggested in literature.

Equations	Condition	Recommended by
$k = \frac{\sum_{j=1}^{m}(t_j \times p_j)}{t_j^2}$	$0.85 < k < 1.15$	Golbraikh and Tropsha (2002)
$k' = \frac{\sum_{j=1}^{m}(t_j \times p_j)}{p_j^2}$	$0.85 < k' < 1.15$	Golbraikh and Tropsha (2002)
$R_m = R^2 \times (1 - \sqrt{\lvert R^2 - R_0^2 \rvert})$ where	$R_m > 0.5$	Roy and Roy (2008)
$R_o^2 = 1 - \frac{\sum_{j=1}^{m}(p_j - t_j^o)^2}{\sum_{j=1}^{m}(p_j - \overline{p_j^o})^2}; t_j^o = k \times p_j$	$R_o^2 \cong 1$	
$R_o'^2 = 1 - \frac{\sum_{j=1}^{m}(t_j - p_j^o)^2}{\sum_{j=1}^{m}(t_j - \overline{t_j^o})^2}; p_j^o = k' \times t_j$	$R_o'^2 \cong 1$	

is estimated using two separate machine learning techniques namely as gene expression programming (GEP) and random forest (RF). These methods are selected for the reliability and robustness of their prediction and their role as specialists in machine learning techniques in related works.

3.1. GEP

GEP is a comparatively new modeling technique that has proven superior modeling in terms of achieving explicit formulations for laboratory trials to traditional regression approaches and neural networks (Rajaee et al., 2020). The programming of GEP is close to that of genetic programming (GP) and genetic algorithms (GAs), since it often uses samples of people, selects fitness from them and incorporates genetic diversity by using one or more genetic operators (Faradonbeh et al., 2018). GEP is a form of an evolutionary algorithm incorporating both linear, fixed-long chromosomes of genetic algorithms and expression parses of various genetic programming shapes and sizes (Baykasoğlu et al., 2008). The programming language of GEP is karva, which is equivalent to LISP (Mahdinia et al., 2019).

GEP genes are all identical in length but these fixed-length genes will code various sizes and shapes for expression trees (ET) (Ferreira, 2001). These separate genes remain united to construct a chromosome through the use of the connection functions (Hashmi et al., 2011). ETs include operators, functions, constants and variables (Peng et al., 2014). The GEP program uses addition, subtraction with multiplication and division as connecting functions. A single gene chromosome can be chosen to solve a query, and then modeling can be carried out with the addition of head weight (Güllü, 2017). But the number of genes can increase and a feature to connect the sub-expression trees (sub-ETs) can be chosen if it is very high (Poli, 2001). Fig. 3 illustrates the flow diagram of the GEP algorithm. The algorithm begins with the random production of chromosomes of a fixed length for each person. Then they are like expression trees (ETs). Each individual will then be assessed for fitness (Ferreira, 2001). The reiteration starts with different people for many generations, until the finest result is reached. Genetic function as mutation, reproduction and crossover is performed for the reiteration of the population (Chelouah and Siarry, 2000).

3.2. Random forest

In RF approaches, a mathematical model to storage data in data is based on a method of decision-making trees (DT) that constitute the decision-making framework on the basis of information theory (Rokach and Maimon, 2014). DT can be used to make predictions about categorical or continuous data. Accurate methodology of the DT algorithm varies slightly depends on whether tasks are being performed for classification (categorical predictions) or regression (continuing prediction) (Nilsen et al., 2019). This topic will concentrate on regression DT, since regression was employed for this study. Regression DT can be considered as part-specific regressions, where the exact regression equal used for predicting a particular data point is based on the values of the data point

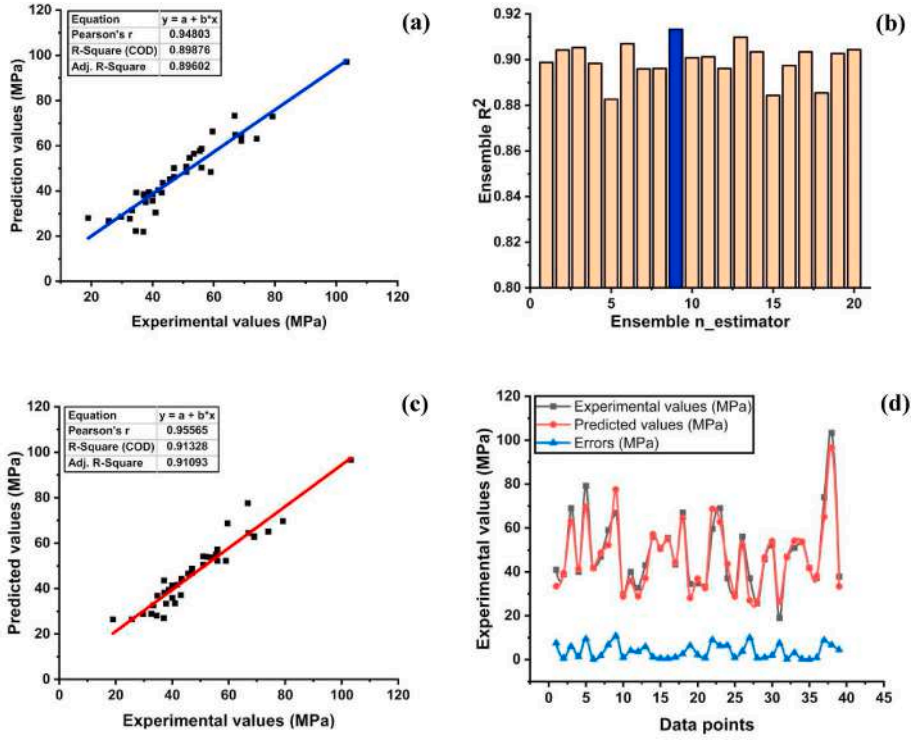

Fig. 6. (a) Individual model prediction; (b) ensemble model with 20 sub-models; (c) ensemble model prediction; (d) ensemble model prediction error between target and predicted values.

Table 5
Models prediction of testing set.

S. No	Experimental values (MPa)	Individual model (MPa)	RF ensemble model (MPa)	Experimental values (MPa)	GEP model (MPa)
1	52.1	54.66	54.0278	25.70	25.72
2	103.3	97.13	96.6411	57.30	57.59
3	56	50.33	52.2011	39.50	39.86
4	34.5	22.28	28.1411	27.40	26.72
5	19	28.06	26.44	72.70	73.43
6	59	48.42	52.2189	52.10	52.90
7	51	50.72	54.1789	32.60	33.52
8	51	48.47	50.4344	51.00	52.04
9	40	35.71	35.9244	35.30	36.35
10	32.6	27.76	28.92	29.70	28.58
11	37.8	35.1	33.3633	31.10	32.22
12	37	21.96	27.0056	33.30	32.12
13	74	63.14	65.1	41.80	40.61
14	25.7	26.81	26.4578	55.30	54.04
15	67	64.85	64.4278	52.60	54.07
16	29.7	28.61	28.8278	29.70	28.22
17	59.6	66.36	68.7044	56.50	58.08
18	55.5	57.8	54.9833	40.00	41.89
19	43	39.27	37.1356	32.40	34.46
20	41	30.5	33.4744	22.70	24.80
21	56	58.7	57.1533	47.00	44.85
22	45.7	45.16	46.6111	57.60	59.83
23	47	46.2	46.7744	51.40	49.03
24	38.8	39.46	39.4022	35.10	37.73
25	37.2	38.11	38.1311	60.80	57.99
26	69	62.19	62.6922	46.80	49.67
27	43.3	43.67	44.3178	45.20	48.33
28	66.8	73.25	77.5667	51.00	47.86
29	69	64.35	63.0178	27.60	31.16
30	79.2	72.95	69.71	56.00	52.41
31	34.7	39.29	36.8856	40.80	36.92
32	53.5	56.5	53.7689	16.00	12.05
33	33.3	31.47	32.5922	72.80	76.90
34	37.1	38.59	43.5844	59.00	54.64
35	41.8	40.34	41.6589	62.00	57.63
36	29.7	28.61	28.8278	60.00	55.61
37	40	38.57	41.3678	67.20	71.67
38	41.8	40.34	41.6589	64.00	68.48
39	47	50.16	48.73	47.00	42.51

features and the tree structure (Xu et al., 2005). The predictions shall be made by DT from the root node of the tree to the leaf nodes (Sivakami, 2021). In contrast, Breiman recommended in 2001 an enhanced regression method called as random forest regression (RFR) (Babar et al., 2020). The RF technique consists of three main steps including assembling training data sets of trained regression trees, calculating the mean value of a single regression tree result and validating the results through the validation data sets (Fouilloy et al., 2018). A new trained dataset of boot-strap information is used to calculate the original trained set. Some data points are deleted and exchanged with current data points in this step. The data points that have been removed from other data sets are called data points that are not included in the bag (di Laurea di Edoardo Giovanni Colombo Matricola et al., 2014). The regression function is then estimated by 2/3rd of the data points and the out-of-bag data points are used for the model validation. This process continues until the necessary accuracy is achieved (Debasish Saha Roy et al., 2019). The RFR is an integrated process which deletes and uses the data points for validation from out-of-bag data points. This is the characteristic feature of RFR. Finally, a total error is calculated for each tree of expression that shows each tree's efficiency and accurateness (Cheng et al., 2019). Flexibility and speed in developing the connection among both output and input variables are the primary features of RFR (Gong et al., 2018). In addition to other machine learning algorithms, random forest controls large data sets more efficiently. In several sectors, such as pharmaceutical and medicine production, banking, customer response prevision and stock pricing etc, it has been used (Cooke, 2005). It was also used for a variety of engineering fields including potential groundwater mapping using system based (GIS-) data (Hornik et al., 2003), high strength concrete (Han et al., 2019), light-weight self--compactant concrete (Zhang et al., 2019), high-performance concrete compressive strength forecast (Erdal, 2013) etc.

4. Data collection

The central element in the design and analysis of concrete is compressive strength (fc'). The creation of a reliable and accurate model for RHA-based concrete is based on input variables and data points. Comprehensive data points are taken from the published literature as shown in Annexure A. The variables used in modeling for RHA-based concrete consist of age (days), cement (Kg/m^3), rice husk ash (Kg/m^3), water (Kg/m^3), super plasticizer (Kg/m^3) and aggregate (Kg/m^3). The frequency distribution and descriptions of overall data used in making model is shown in Fig. 4 and Table 2. Moreover, the distribution of explanatory variables over a large range ensures the model's best performance (Khan et al., 2021b). The interdependence of the certain parameters used in making model must be examined to prevent complication in model interpretation. This correlation problem between selected parameters is referred as multi-collinearity. For this, the correlation coefficient between two variables must be less than 0.8 in order to mitigate and to give benignant effect in making model (Corotis, 1988). Table 3 represents that the entire variable used in model show lesser correlation with negative and positive values. Moreover, the compressive strength of RHA concrete is influenced significantly by all the variables selected.

5. K-Fold cross validation and statistical checks

Cross-validation is a mathematical practice for assessing the efficiency of the models used to avoid over fitting and biasness in training set data. It divides the entire data set into k^{10}-data sub-sets with one set as testing set (k^1) out of ten, and remaining set ($k^{10\text{-}1}$) used for training of the model (Saud et al., 2020). Kohavi's (Kohavi, 1995) proposed that KFCV result in accurate variance and is better suited for optimal calculation time. This research evaluates and validates both models by using K^{10} subset as illustrated in Fig. 5.

Moreover, statistical checks are employed to evaluate model effectiveness and accuracy. These statistical measures include mean absolute error (MAE), coefficient of determination (R2), performance index (ρ), root man square error (RMSE), relative squared error (RSE) and relative root mean square (RRMSE) (see equations (1)–(6)).

$$R^2 = 1 - \frac{\sum_{j=1}^{m}(p_j - t_j)^2}{\sum_{j=1}^{m}(t_j - \bar{t})} \tag{1}$$

$$RMSE = \sqrt{\frac{\sum_{j=1}^{m}(t_j - p_j)^2}{n}} \tag{2}$$

$$RRMSE = \frac{1}{|\bar{t}|}\sqrt{\frac{\sum_{j=1}^{m}(t_j - p_j)^2}{n}} \tag{3}$$

$$MAE = \frac{\sum_{j=1}^{m}|t_j - p_j|}{n} \tag{4}$$

$$RSE = \frac{\sum_{j=1}^{m}(p_j - t_j)^2}{\sum_{j=1}^{m}(\bar{t} - t_j)^2} \tag{5}$$

$$\rho = \frac{\mathrm{RRMSE}}{1 + \sqrt{R^2}} \tag{6}$$

Where.

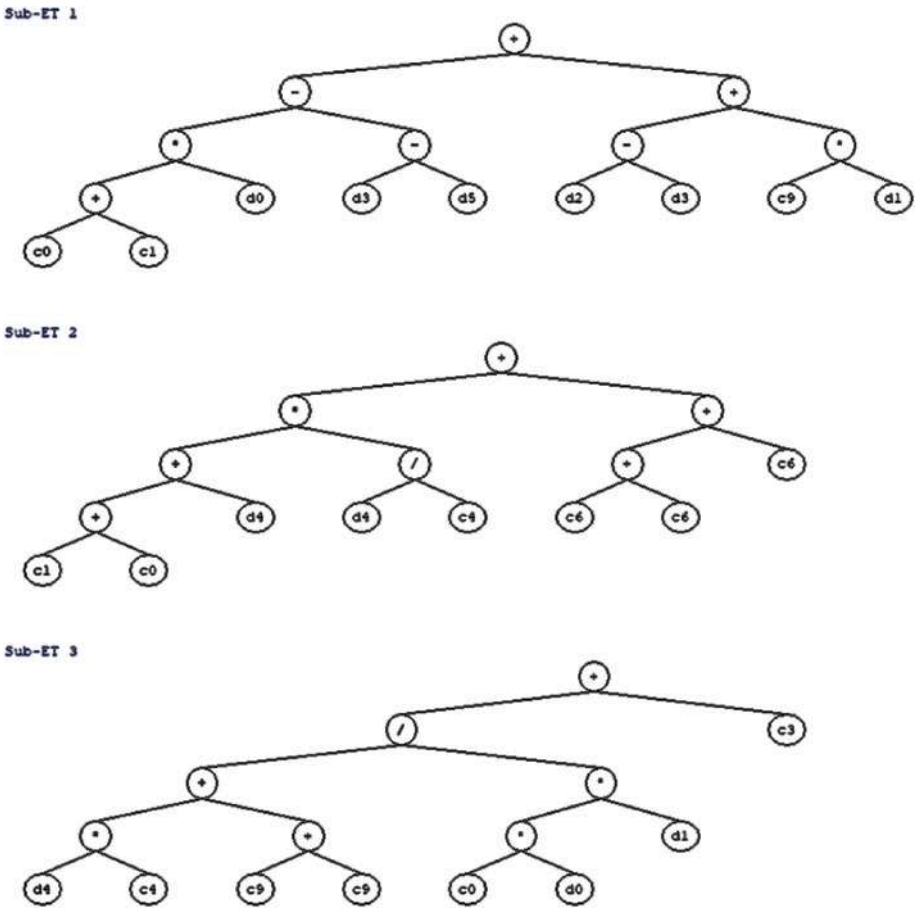

Fig. 7. RHA based Expression tree with variables and constants.

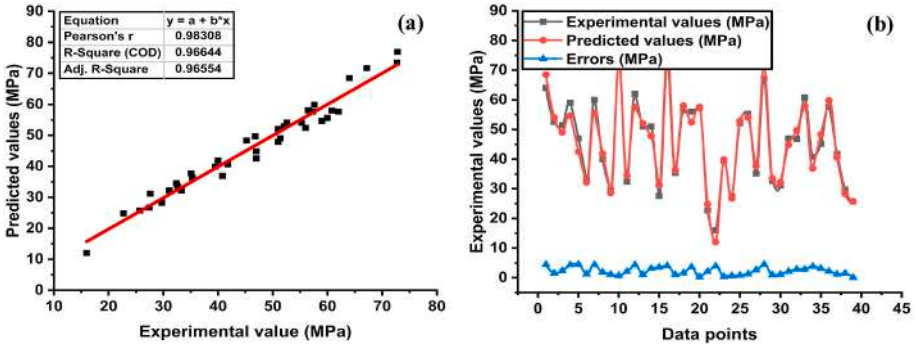

Fig. 8. (a) Experimental vs model regression based on GEP model; (b) Errors between experimental and targets values based on GEP model.

t_j = experimental values before making model.
p_j = predicted outcome from the model.
$\bar{t}_j$ = represent the target mean value.
$\bar{p}_i$ = represent the predicted mean value.
m = refers to the total number of instances used in modeling.

The higher value of coefficient of determination R^2 and lower value of statistical error represents an optimum and reliable model (Nguyen et al., 2019). Also, model accurateness is also evaluated by it R^2 value. Literature suggests that R^2 value ranges from 0 to 0.5 represents fair model and 0.5 to 0.8 represents good model. However, R^2 value greater than 0.8 shows that there exists a linear and strong relationship with less errors that depicts a superior model (Gandomi et al., 2011). As R^2 cannot be used solely as a metric for the general effectiveness of the model, since it is insensitive to division or the multiplication of results to a constant (Jalal et al., 2021). The MAE and RMSE also list the size and significance of the average error. In RMSE, the error values are squared even before averages are computed and thus useful for interpreting larger errors. Whereas, MAE assigns small weighted values to larger errors. A high RMSE shows a high error in the large number of expected results and must be omitted. Despotovic et al. (2016) classify the model as good and outstanding, if the RRMSE values range from 0 to 0.11 and 0.11 to 0.20 respectively (Despotovic et al., 2016). The values of ρ must go from 0 to infinity. Also, for a successful model ρ should be less than 0.2 recommended by Gandomi et al. (2015). It should be noted that ρ covers both factors (RRMSE and R) at the same time. Thus, the value of $\ddot{\rho}$ should be close to 0 for superior model efficiency. In addition, this research paper also considers various statistical methods for the validity

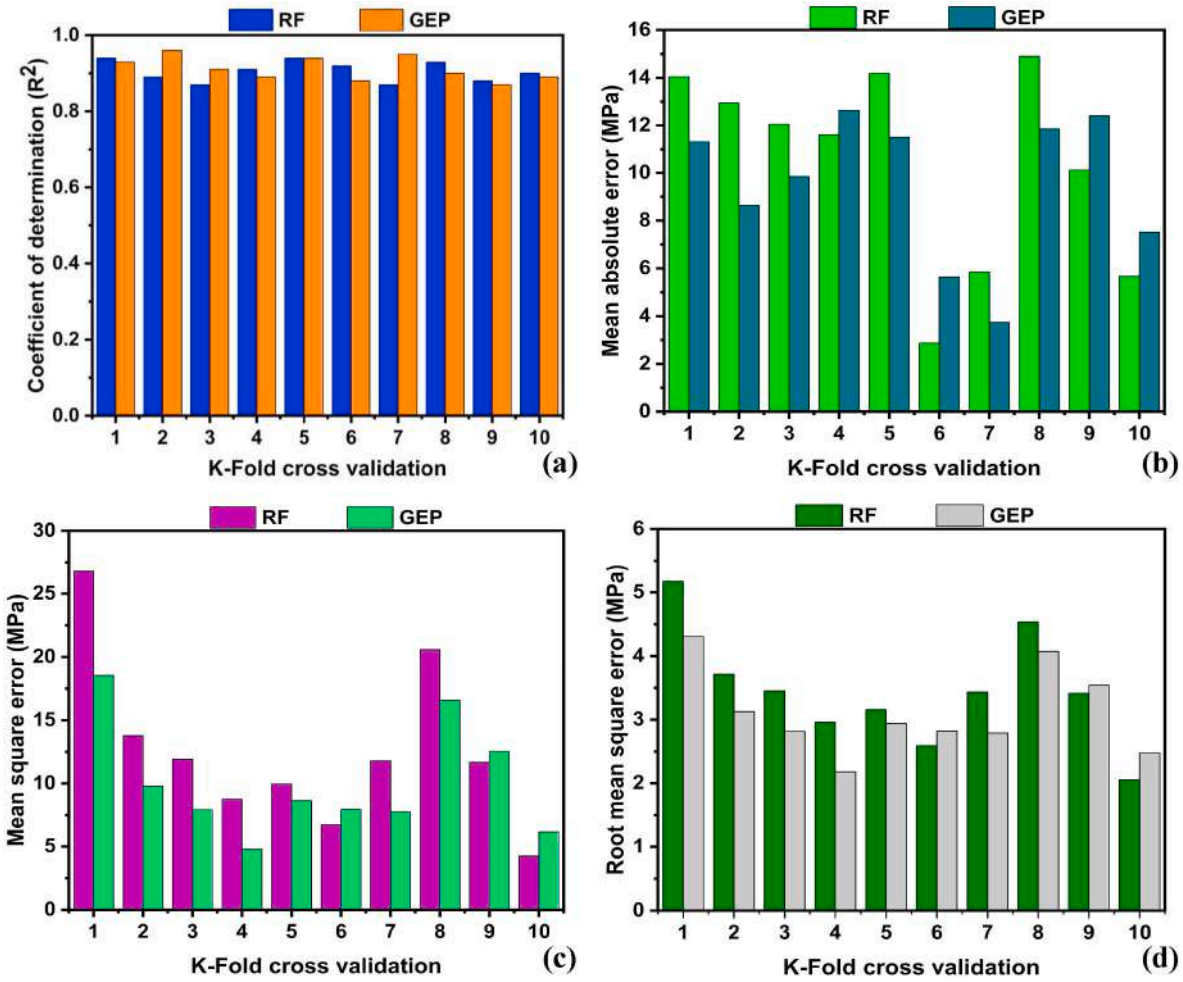

Fig. 9. K-fold cross validation; (a) R^2 validtion; (b) MAE validation; (c) MSE validation; (d) RMSE validation.

Table 6
K-Fold cross validation of models.

K-Fold	RFR model				GEP Model			
	R^2	MAE (MPa)	RMSE (MPa)	MSE (MPa)	R^2	MAE (MPa)	RMSE (MPa)	MSE (MPa)
1	0.94	14.04	5.17	26.7651	0.93	11.31	4.31	18.54
2	0.89	12.94	3.71	13.7808	0.96	8.64	3.13	9.7808
3	0.87	12.05	3.45	11.9242	0.91	9.84	2.81	7.9242
4	0.91	11.61	2.96	8.75747	0.89	12.64	2.18	4.75747
5	0.94	14.18	3.16	9.96117	0.94	11.51	2.94	8.64
6	0.92	2.87	2.59	6.71695	0.88	5.64	2.82	7.95
7	0.87	5.84	3.43	11.7837	0.95	3.74	2.79	7.7837
8	0.93	14.90	4.54	20.5789	0.9	11.85	4.07	16.5789
9	0.88	10.12	3.41	11.6615	0.87	12.41	3.54	12.54
10	0.9	5.66	2.06	4.23181	0.93	11.31	2.48	6.14
Maximum	0.94	14.90	5.17	26.76	0.96	12.64	4.31	15.84
Minimum	0.87	2.87	2.057	4.23	0.87	3.74	2.182	4.75
Mean	0.905	10.42	3.449	12.616	0.912	9.509	3.10	10.06

Table 7
Summary of statistical error checks and performance index.

Developed models	R^2	MAE (MPa)	RMSE (MPa)	RRMSE	RSE (MPa)	Sigma
GEP	0.967	2.29	2.677	0.058	0.035	0.029
RFR	0.913	3.751	4.973	0.103	0.092	0.052

Table 8
Summary of Statistical metrics suggested in literature.

Suggested Metric	RFR model	GEP model
k	0.982	0.996
k'	1.030	1.009
R_m	0.648	0.789
R_o^2	0.997	0.999
$R_o'^2$	0.991	0.999

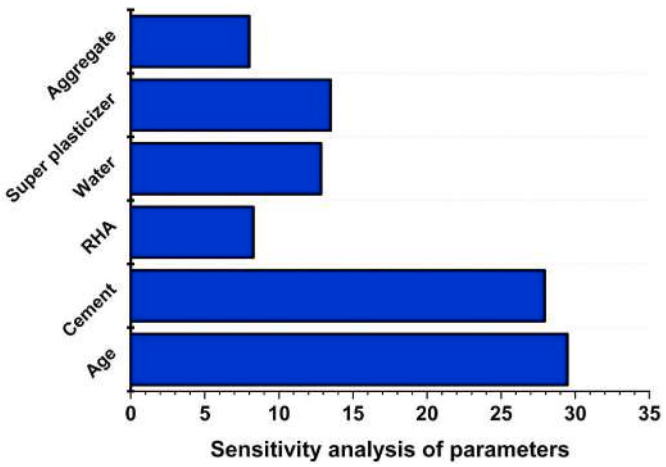

Fig. 10. Sensitivity analysis of parameters.

of the model as proposed in the literature (see Table 4).

6. Result and discussion

6.1. RF result

The prediction of RHA concrete using a random forest algorithm gives a clear relation between experimental strength values and modeled strength as shown in Fig. 6. It can be seen that RF without optimization gives a better accuracy with $R^2 = 0.89$ with less variance as illustrated in Fig. 6(a). Moreover, the model is optimized by making twenty sub-models, which depicted that ninth model yields maximum accuracy with $R^2 = 0.913$ as compared to other models as shown in Fig. 6(b). Also, their relation with target to prediction with $R^2 = 0.913$ is illustrated in Fig. 6(c). The overall response of the model has been significantly improved following the ensemble approach. This is attributed to the increased reliability of the model as a result of the use of weak base learners taking multiple data to form the right model (Khan et al., 2021a). The overall response of the RF algorithm for the RHA based experimental data can also be evaluated with respect to errors as illustrated in Fig. 6(d). It shows that the test set data model with RFR gives an average error of about 3.75 MPa with minimum and maximum error as 0.14 MPa, and 10.76 MPa respectively. Moreover, 97% error of the model lies below 10 MPa which depict the overall accuracy of the entire model. Table 5 represents the detail results of the RF model.

6.2. Formulation of RHA empirical equation using GEP

The GEP algorithm expressed the compressive strength of RHA based concrete by forming an empirical equation from expression trees (ETs) as illustrated in Fig. 7. Four fundamental arithmetic operation is used in sub-ETs namely as, addition (+), subtraction (−), multiplication (x) and division (/) as represented in Fig. 7. These ETs uses different indicators including parameters starting from d_0 to d_5 values and constant values that make empirical relation accurate. Equation (7) represents the ultimate expression that was derived by decoding the ETs.

6.2.1. Performance of GEP model

The relation between the expected RHA based concrete and GEP predicted values for the training subset is illustrated in Fig. 8. It shows clearly that GEP model correlated significantly between targeted and predicted results with $\mathbf{R^2}$**=0.94**. Furthermore, Fig. 8(b) represent the absolute error distribution among actual and GEP results. Moreover, testing set show an average error of about 2.39 MPa with 0.039 MPa, 6.75 MPa as minimum and maximum error. This describes the strong robust performance of the built GEP model and overall response of the model is listed in Table 5.

$$y = y_a / y_b / y_c \tag{7}$$

$$ya = (5.45 * A) - (W - A) + (RHA - W) + (2.22 * C) \tag{7a}$$

$$yb = (-12.45) + SP\left(\frac{SP}{5.29}\right) + (24.46) \tag{7b}$$

$$yc = \left(\frac{34.65*SP + 421.57}{0.20*A*C} + 2.03\right) \tag{7c}$$

Where.

A = age,
W = water
SP = superplasticizer
C = cement

6.3. K-fold cross validation (KFCV)

The robustness of the model based on regression analysis is evaluated by conducting K-Fold cross validation (KFCV) as illustrated in Fig. 9. Thus, various statistical error checks were applied to analyse the model accuracy with KFCV that includes mean square error (MSE), root mean square error (RMSE), and coefficient of determination (R^2) as shown in Fig. 9. Moreover, KFCV ensure the accuracy and reliability of the prediction models. Figure (a) represents the R^2 of GEP with higher validation accuracy with maximum, minimum and average value of 10 K-fold lies in the range of 0.96, 0.87, and 0.912 respectively. Similarly, RFR shows same trend that depict the robust performance of the model with **0.94, 0.87, and 0.905** as maximum, minimum and average value of 10 K-fold validation. In addition, the error value of MSE, RMSE and MAE with 10 K-fold validation is also shown in Fig. 9(b,c,d). This demonstrate that all the statistical indicator show lesser response that depicts higher accurateness of entire models. The overall response of validation result is also listed in Table 6. In addition, model accuracy is also evaluated by conducting statistical analysis check.

Statistical error assessments are also carried out to evaluate the efficiency of the model as illustrated in Table 7. The RMSE, MAE and RSE are significantly lower for both models that mean that models are reliable and accurate in predicting the compressive strength of RHA-based concrete. Moreover from the statistical error check it is found out that GEP showing better predictive results than the RFR.

The model validation can also be evaluated by various external models by conducting statistical analysis as illustrated in Table 8. It can been seen that the k and k ' are closer to 1 for both models thus fulfilling validation criteria (Golbraikh and Tropsha, 2002). The R_m is also higher than 0.5 for both models and fulfils Roy and Roy's suggested criteria (Roy and Roy, 2008). Thus both models give robust performance interm of prediction of compressive strength.

6.4. Sensitivity and parametric analysis

Sensitivity analysis (SA) is conducted on the GEP model due to its better performance as compared with other models. The relative contribution of variables to the outcome is determined by the sensitivity analysis (SA). The following equations are used to mathematically implement SA:

$$N_i = f_{max}(x_i) - f_{min}(x_i) \tag{8}$$

$$SA = \frac{N_i}{\sum_n^{j=1} N_j} \tag{9}$$

Where.

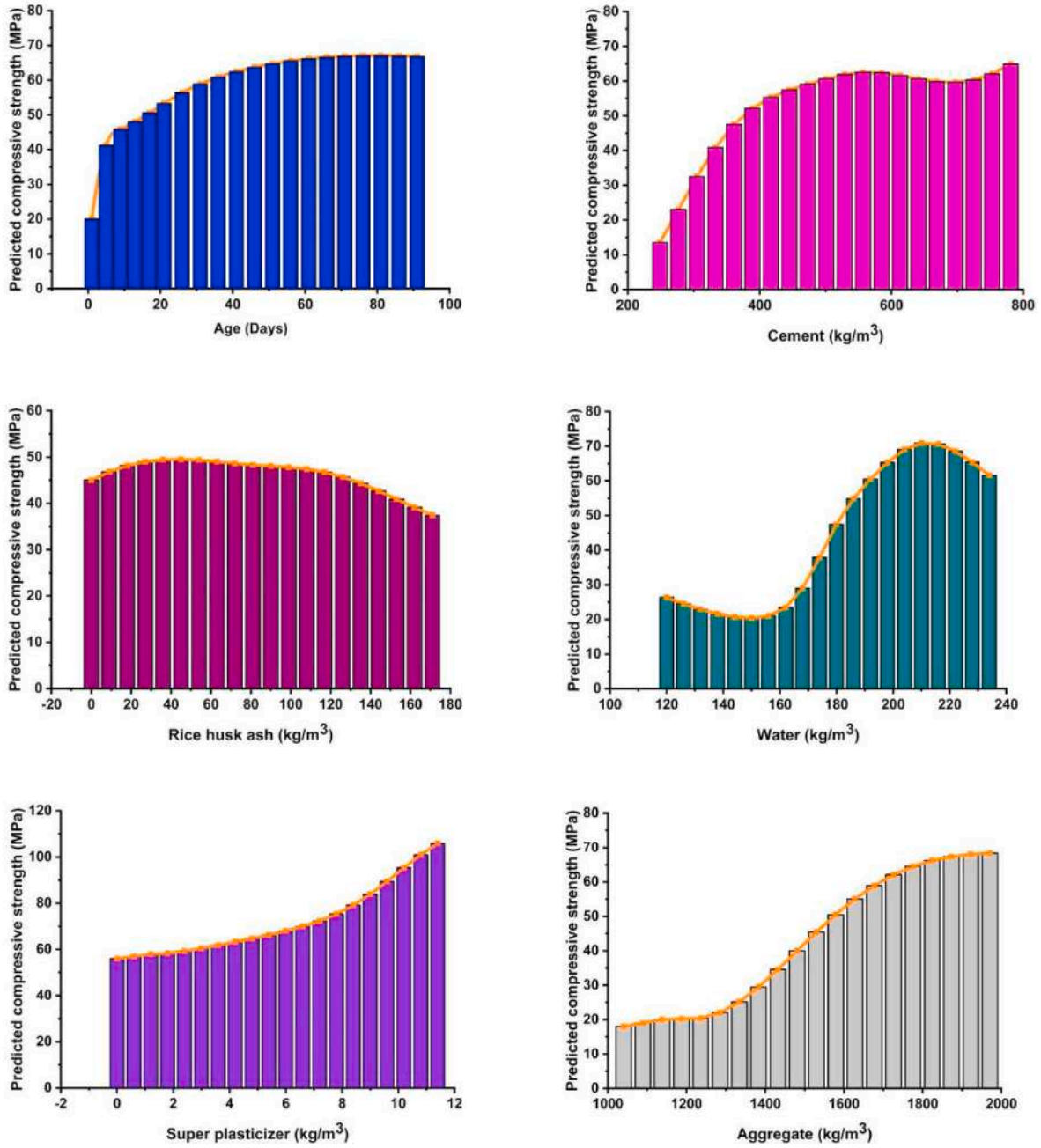

Fig. 11. Parametric analysis of inputs; (a) age (kg/m^3), (b) cement (kg/m^3), (c) rice husk ash (kg/m^3), (d) water (kg/m^3), (e) superplasticizer, (f) aggregate.

$f_{min}(x_i)$ = minimum output of the predicted model
$f_{max}(x_i)$ = maximum output of the predicted model
i = representing the domain of the input variables and keeping other variables constant

It can be seen in Fig. 10 that every parameter plays a vital role in prediction of compressive strength of RHA. From sensitivity analysis it can be seen that age and cement plays an important role in overall contribution of the compressive strength which turns out to be more than 50%. The age contributes almost 29.47% while cement contributes about 27.93%. The rest of the four parameters i.e. RHA, water, SP and aggregate contribute about 8.26%, 12.85%, 13.49% and 7.99% respectively.

A parametric analysis (PA) was also conducted in conjunction with sensitivity analysis. This helps to determine the influence of the input parameter on the output parameter. This is done by keeping the entire variables constant at their average value except for one variable. Moreover, changes in the compressive strength occur when one input variable varies from its lowest to its highest value as illustrated in Figure. It can be seen that the number of days, super plasticizer and aggregate shows a similar increasing trend. However, water and RHA show increase and then decrease behavior (see Fig. 11). The decrease in compressive strength is due to as workability depends mostly on the ratio of water and cement. Furthermore, too much water mixing is likely the most critical reason for many issues, such as reducing the compression strength of concrete (Rao, 2001; Yaşar et al., 2004). Similarly, concrete incorporating RHA needs more water than concretes having only Portland cement due to high specific surface area. Bheel et al. (2018) investigated the RHA effect with W/C ratio on strength and report a decrease in strength by increasing the W/C ratio. Compressive strength was decreased for w/c ratio of 0.60. However, compressive strength depicted maximum value for w/c ratio of 0.45. Similarly,

Nagrale et al. (Cheng et al., 2019) discovered that increasing the water content decreases compressive strength. Furthermore, because of its filler and silica impact, RHA contributes to increased strength. However, increasing the RHA concentration over 30% results in a reduction in compressive strength. This is because RHA comprises 90 percent of silica content, increasing amount shows unreacted particles which ultimately decrease its strength (Ramezanianpour et al., 2009).

7. Conclusions

1. This study utilized GEP and RFR (individual and ensemble) model to predict the compressive strength of RHA concrete. An extensive and reliable data base of 192 points was collected and employed in the development of the models. Following conclusions of the study can be drawn from the developed models. 1. RHA concrete prediction utilising a GEP yields a significant link between the experimental and modeling strength values, with a regression relation of R2 = 0.966, compared to RFR, which yields R2 = 0.89 for the individual model and R2 = 0.91 for the ensemble approach.
2. Empirical equation is developed using GEP model and can be utilized to determine the compressive strength of RHA concrete.
3. Ensemble and individual models were developed using RFR algorithm. Optimization of RFR was made with twenty models. However, ninth ensemble model gives $R^2 = 0.91$ with an enhancement of 1.62 as compared to individual RFR model..
4. GEP model depicts an enhancement of 37.3 percent in average error with value of 2.39 MPa, whereas RFR illustrates an average error of 3.75 MPa.
5. When compared to the RFR model, cross validation of the GEP model yields greater validation accuracy using different statistical tests. Furthermore, statistical and external validation show that the GEP model performs well, with fewer errors and a high correlation coefficient..
6. The parametric analysis demonstrates that compressive strength is adequately predicted by the model utilising the input parameters, with cement and age being the key influences in this research.

8. Future recommendation

The concrete with RHA can replace ordinary Portland cement concrete with high potential. Extensive study for RHA by including more parameters is recommended. To provide a more general expression, including more input parameters and extending the database can provide more reliable results. Temperature, acid attack resistance, chloride resistance, sulphate resistance and corrosion should be included in these factors. For further predictions further advanced methods such as the programming of particle swarm optimization (PSO) and M5P tree can be applied.

However, in addition, ML techniques can be combined with heuristic methods, including whale optimization algorithm, ant colony optimization, and particle swarm optimization, for better results. These methods can then be compared with the techniques employed in this study. Moreover, multiexpression programming (MEP) is an extended and improved form/version of GEP. GEP and MEP analysis should be employed and compared to overcome the limitations of ensemble algorithms.

Author contributions

B.I.: Data curation and Writing - original draft. **S.C.A.:** Project administration & Funding acquisition. **M.V.:** Conceptualization, validation & Supervision; **M.A.E.:** Formal analysis, Methodology, writing, review, and editing. **M.S..:** Software, funding, writing, review, and editing. **M.F.J.:** Visualization, writing - review & editing. **W.D.:** Investigation, writing - review & editing. **M.I.K.:** Resources, writing, review and editing. **F.A.:** Methodology, writing, review, and editing.

Declaration of competing interest

The authors declare that they have no known competing financial interests or personal relationships that could have appeared to influence the work reported in this paper.

Acknowledgments

The authors extend their appreciation to the Deanship of Scientific Research at King Khalid University, Abha, Saudi Arabia, for funding this work through the Research Group Program under grant no. RGP. 2/19/43.

The authors would like to thank the Ministry of Higher Education of Malaysia and Universiti Teknologi Malaysia for their financial support through research grants vote number of 5F365 and 16J24.

Annexure-A.

S.No.	A	Cem	RHA	W	SP	FA	Exp.
1	1	495	55	165	5.8	1819	22.7
2	1	500	0	160	5.5	1891	20.9
3	1	400	100	160	6.22	1859	22
4	1	425	75	170	5	1843	19.7
5	1	495	55	165	6.8	1819	34.7
6	1	500	0	160	6.5	1891	37.8
7	1	400	100	160	7.36	1859	34.2
8	1	425	75	170	6.4	1843	32.6
9	3	495	55	165	5.8	1819	47.9
10	3	500	0	160	5.5	1891	41.3
11	3	400	100	160	6.22	1859	48.7
12	3	425	75	170	5	1843	45.2
13	3	378	42	189	0	1810	17.6
14	3	495	55	165	6.8	1819	60.8
15	3	500	0	160	6.5	1891	63.9
16	3	400	100	160	7.36	1859	60.7
17	3	425	75	170	6.4	1843	57.3
18	7	495	55	165	5.8	1819	60.6
19	7	500	0	160	5.5	1891	51
20	7	400	100	160	6.22	1859	61.8
21	7	375	0	150	0	1970	30

(continued on next page)

(*continued*)

S.No.	A	Cem	RHA	W	SP	FA	Exp.
22	7	356.25	18.75	142.5	0	1970	31.5
23	7	337.5	37.5	135	0	1970	32.5
24	7	318.75	56.25	127.5	0	1970	35.5
25	7	300	75	120	0	1970	31
26	7	364	19	203	0	1725	27.6
27	7	306	77	203	0	1725	29.7
28	7	249	134	203	0	1725	25.7
29	7	425	75	170	5	1843	57.6
30	7	495	55	165	6.8	1819	83.6
31	7	391	29	189	0	1810	32.4
32	7	500	0	160	6.5	1891	76.4
33	7	400	100	160	7.36	1859	82.8
34	7	425	75	170	6.4	1843	79.2
35	14	345	38	203	0	1725	35.3
36	14	287	96	203	0	1725	36.1
37	28	495	55	165	5.8	1819	72.8
38	28	500	0	160	5.5	1891	59.6
39	28	400	100	160	6.22	1859	72.7
40	28	375	0	150	0	1970	44.5
41	28	356.25	18.75	142.5	0	1970	45.5
42	28	337.5	37.5	135	0	1970	49.5
43	28	318.75	56.25	127.5	0	1970	50
44	28	300	75	120	0	1970	43
45	28	383	0	203	0	1725	37.1
46	28	326	57	203	0	1725	41.8
47	28	268	115	203	0	1725	37.6
48	28	425	75	170	5	1843	67.2
49	28	495	55	165	6.8	1819	95.2
50	28	500	0	160	6.5	1891	85.7
51	28	400	100	160	7.36	1859	94.3
52	28	420	0	189	0	1810	40.3
53	28	357	63	189	0	1810	46.9
54	28	425	75	170	6.4	1843	90.3
55	56	375	0	150	0	1970	51.5
56	56	356.25	18.75	142.5	0	1970	53.5
57	56	337.5	37.5	135	0	1970	56
58	56	318.75	56.25	127.5	0	1970	59.5
59	56	300	75	120	0	1970	52
60	90	495	55	165	5.8	1819	83.2
61	90	500	0	160	5.5	1891	66.8
62	90	400	100	160	6.22	1859	82.2
63	90	425	75	170	5	1843	75.8
64	90	364	19	203	0	1725	43.3
65	90	306	77	203	0	1725	46
66	90	249	134	203	0	1725	37.2
67	90	375	0	150	0	1970	55.5
68	90	356.25	18.75	142.5	0	1970	56.5
69	90	337.5	37.5	135	0	1970	63
70	90	318.75	56.25	127.5	0	1970	64
71	90	300	75	120	0	1970	61
72	90	378	42	189	0	1810	59
73	90	495	55	165	6.8	1819	104.1
74	90	500	0	160	6.5	1891	94
75	90	400	100	160	7.36	1859	103.3
76	90	425	75	170	6.4	1843	99.1
77	7	481	48.1	169.312	3.367	1040	39.5
78	7	427	85.4	163.968	3.416	1040	30.5
79	7	416	41.6	183.04	1.1232	1041	29.7
80	7	370	74	177.6	1.85	1041	23.6
81	7	367	36.7	201.85	1.101	1041	22.7
82	7	327	65.4	196.2	1.308	1041	20.8
83	28	481	48.1	169.312	3.367	1040	51.4
84	28	427	85.4	163.968	3.416	1040	47.4
85	28	416	41.6	183.04	1.1232	1041	40.8
86	28	370	74	177.6	1.85	1041	39.4
87	28	367	36.7	201.85	1.101	1041	34.5
88	28	327	65.4	196.2	1.308	1041	35.9
89	90	481	48.1	169.312	3.367	1040	64.5
90	90	427	85.4	163.968	3.416	1040	68.5
91	90	416	41.6	183.04	1.1232	1041	51.5
92	90	370	74	177.6	1.85	1041	57.3
93	90	367	36.7	201.85	1.101	1041	44.4
94	90	327	65.4	196.2	1.308	1041	52.9
95	1	450	0	238	11.25	1405	31.5
96	1	427.5	21.375	238	10.6875	1405	32.1
97	1	405	40.5	238	10.125	1405	33.3

(*continued on next page*)

(*continued*)

S.No.	A	Cem	RHA	W	SP	FA	Exp.
98	1	382.5	57.375	238	9.5625	1405	34.5
99	1	360	72	238	9	1405	33.6
100	1	337.5	84.375	238	8.4375	1405	29.3
101	1	315	94.5	238	7.875	1405	29
102	28	450	0	238	11.25	1405	41.7
103	28	427.5	21.375	238	10.6875	1405	42.7
104	28	405	40.5	238	10.125	1405	44.2
105	28	382.5	57.375	238	9.5625	1405	46.8
106	28	360	72	238	9	1405	43.5
107	28	337.5	84.375	238	8.4375	1405	39.5
108	28	315	94.5	238	7.875	1405	38.2
109	56	450	0	238	11.25	1405	49.1
110	56	427.5	21.375	238	10.6875	1405	50.2
111	56	405	40.5	238	10.125	1405	52.1
112	56	382.5	57.375	238	9.5625	1405	55.3
113	56	360	72	238	9	1405	55.2
114	56	337.5	84.375	238	8.4375	1405	47
115	56	315	94.5	238	7.875	1405	45.9
116	90	450	0	238	11.25	1405	52.6
117	90	427.5	21.375	238	10.6875	1405	54.9
118	90	405	40.5	238	10.125	1405	57.3
119	90	382.5	57.375	238	9.5625	1405	61.2
120	90	360	72	238	9	1405	55.5
121	90	337.5	84.375	238	8.4375	1405	51.9
122	90	315	94.5	238	7.875	1405	50.2
123	1	783	87	212	3.6	1277	41
124	1	571	0	219	1	1566	30
125	1	514	57	218	1.4	1541	27
126	1	457	114	216	2.6	1515	26
127	1	400	171	215	3.7	1490	19
128	1	383	42	221	0.3	1670	16
129	3	783	87	212	3.6	1277	59
130	3	571	0	219	1	1566	46
131	3	514	57	218	1.4	1541	41
132	3	457	114	216	2.6	1515	38
133	3	400	171	215	3.7	1490	32
134	3	383	42	221	0.3	1670	26
135	7	783	87	212	3.6	1277	62
136	7	571	0	219	1	1566	50
137	7	514	57	218	1.4	1541	47
138	7	457	114	216	2.6	1515	47
139	7	400	171	215	3.7	1490	43
140	7	383	42	221	0.3	1670	37
141	14	783	87	212	3.6	1277	63
142	14	571	0	219	1	1566	54
143	14	514	57	218	1.4	1541	52
144	14	457	114	216	2.6	1515	52
145	14	400	171	215	3.7	1490	51
146	14	383	42	221	0.3	1670	40
147	28	783	87	212	3.6	1277	66
148	28	571	0	219	1	1566	56
149	28	514	57	218	1.4	1541	61
150	28	457	114	216	2.6	1515	60
151	28	400	171	215	3.7	1490	54
152	28	383	42	221	0.3	1670	47
153	56	783	87	212	3.6	1277	69
154	56	571	0	219	1	1566	60
155	56	514	57	218	1.4	1541	62
156	56	457	114	216	2.6	1515	61
157	56	400	171	215	3.7	1490	60
158	56	383	42	221	0.3	1670	51
159	90	783	87	212	3.6	1277	74
160	90	571	0	219	1	1566	67
161	90	514	57	218	1.4	1541	67
162	90	457	114	216	2.6	1515	69
163	90	400	171	215	3.7	1490	64
164	90	383	42	221	0.3	1670	56
165	7	364	19	203	0	1725	27.6
166	7	345	38	203	0	1725	28
167	7	326	57	203	0	1725	29.3
168	7	306	77	203	0	1725	29.7
169	7	287	96	203	0	1725	28.7
170	7	268	115	203	0	1725	27.4
171	7	249	134	203	0	1725	25.7
172	14	364	19	203	0	1725	34.2
173	14	345	38	203	0	1725	35.3

(*continued on next page*)

(*continued*)

S.No.	A	Cem	RHA	W	SP	FA	Exp.
174	14	326	57	203	0	1725	36
175	14	306	77	203	0	1725	39.3
176	14	287	96	203	0	1725	36.1
177	14	268	115	203	0	1725	33.5
178	14	249	134	203	0	1725	31.1
179	28	364	19	203	0	1725	40
180	28	345	38	203	0	1725	41.3
181	28	326	57	203	0	1725	41.8
182	28	306	77	203	0	1725	42.5
183	28	287	96	203	0	1725	38.8
184	28	268	115	203	0	1725	37.6
185	28	249	134	203	0	1725	35.1
186	90	364	19	203	0	1725	43.3
187	90	345	38	203	0	1725	44.8
188	90	326	57	203	0	1725	45.7
189	90	306	77	203	0	1725	46
190	90	287	96	203	0	1725	43
191	90	268	115	203	0	1725	38.7
192	90	249	134	203	0	1725	37.2

References

Abu Yaman, M., Abd Elaty, M., Taman, M., 2017. Predicting the ingredients of self compacting concrete using artificial neural network. Alex. Eng. J. 56, 523–532. https://doi.org/10.1016/j.aej.2017.04.007.

Ahmad, A., Farooq, F., Niewiadomski, P., Ostrowski, K., Akbar, A., Aslam, F., Alyousef, R., 2021. Prediction of compressive strength of fly ash based concrete using individual and ensemble algorithm. Materials 14, 794. https://doi.org/10.3390/ma14040794.

Al-Mughanam, T., Aldhyani, T.H.H., Alsubari, B., Al-Yaari, M., 2020. Modeling of compressive strength of sustainable self-compacting concrete incorporating treated palm oil fuel ash using artificial neural network. Sustain 12, 1–13. https://doi.org/10.3390/su12229322.

Aprianti S, E., 2017. A huge number of artificial waste material can be supplementary cementitious material (SCM) for concrete production – a review part II. J. Clean. Prod. 142, 4178–4194. https://doi.org/10.1016/j.jclepro.2015.12.115.

Arrigoni, A., Panesar, D.K., Duhamel, M., Opher, T., Saxe, S., Posen, I.D., MacLean, H.L., 2020. Life cycle greenhouse gas emissions of concrete containing supplementary cementitious materials: cut-off vs. substitution. J. Clean. Prod. 263, 121465. https://doi.org/10.1016/j.jclepro.2020.121465.

Aslam, F., Farooq, F., Amin, M.N., Khan, K., Waheed, A., Akbar, A., Javed, M.F., Alyousef, R., Alabdulijabbar, H., 2020. Applications of gene expression programming for estimating compressive strength of high-strength concrete. Adv. Civ. Eng. 2020 https://doi.org/10.1155/2020/8850535.

Asteris, P.G., Kolovos, K.G., 2019. Self-compacting concrete strength prediction using surrogate models. Neural Comput. Appl. 31, 409–424. https://doi.org/10.1007/s00521-017-3007-7.

Asteris, P.G., Kolovos, K.G., Douvika, M.G., Roinos, K., 2016. Prediction of self-compacting concrete strength using artificial neural networks. Eur. J. Environ. Civ. Eng. 20, s102–s122. https://doi.org/10.1080/19648189.2016.1246693.

Azimi-Pour, M., Eskandari-Naddaf, H., Pakzad, A., 2020. Linear and non-linear SVM prediction for fresh properties and compressive strength of high volume fly ash self-compacting concrete. Construct. Build. Mater. 230, 117021. https://doi.org/10.1016/j.conbuildmat.2019.117021.

Babar, B., Luppino, L.T., Boström, T., Anfinsen, S.N., 2020. Random forest regression for improved mapping of solar irradiance at high latitudes. Sol. Energy 198, 81–92. https://doi.org/10.1016/j.solener.2020.01.034.

Bai, C., Nguyen, H., Asteris, P.G., Nguyen-Thoi, T., Zhou, J., 2020. A refreshing view of soft computing models for predicting the deflection of reinforced concrete beams. Appl. Soft Comput. J. 97, 106831. https://doi.org/10.1016/j.asoc.2020.106831.

Balf, F.R., Kordkheili, H.M., Kordkheili, A.M., 2020. A new method for predicting the ingredients of self-compacting concrete (SCC) including fly ash (FA) using data envelopment analysis (DEA). Arabian J. Sci. Eng. 1–22. https://doi.org/10.1007/s13369-020-04927-3.

Baykasoğlu, A., Güllü, H., Çanakçi, H., Özbakir, L., 2008. Prediction of compressive and tensile strength of limestone via genetic programming. Expert Syst. Appl. 35, 111–123. https://doi.org/10.1016/j.eswa.2007.06.006.

Belalia Douma, O., Boukhatem, B., Ghrici, M., Tagnit-Hamou, A., 2017. Prediction of properties of self-compacting concrete containing fly ash using artificial neural network. Neural Comput. Appl. 28, 707–718. https://doi.org/10.1007/s00521-016-2368-7.

Ben Chaabene, W., Flah, M., Nehdi, M.L., 2020. Machine learning prediction of mechanical properties of concrete: critical review. Construct. Build. Mater. 260 https://doi.org/10.1016/J.CONBUILDMAT.2020.119889, 119889.

Benhelal, E., Zahedi, G., Shamsaei, E., Bahadori, A., 2013. Global strategies and potentials to curb CO2 emissions in cement industry. J. Clean. Prod. 51, 142–161. https://doi.org/10.1016/j.jclepro.2012.10.049.

Beycioǂlu, A., Emirǂlu, M., Kocak, Y., Subaşi, S., 2015. Analyzing the compressive strength of clinker mortars using approximate reasoning approaches - ANN vs MLR. Comput. Concr. 15, 89–101. https://doi.org/10.12989/cac.2015.15.1.089.

Bheel, N., Meghwar, S.L., Abbasi, S.A., Marwari, L.C., Mugeri, J.A., Abbasi, R.A., 2018. Effect of rice husk ash and water-cement ratio on strength of concrete. Civ. Eng. J. 4, 2373. https://doi.org/10.28991/cej-03091166.

Buchanan, A.H., Levine, S.B., 1999. Wood-based building materials and atmospheric carbon emissions. Environ. Sci. Pol. 2, 427–437. https://doi.org/10.1016/S1462-9011(99)00038-6.

Bušić, R., Benšić, M., Miličević, I., Strukar, K., 2020. Prediction models for the mechanical properties of self-compacting concrete with recycled rubber and silica fume. Materials 13, 1821. https://doi.org/10.3390/MA13081821.

Cao, X., Li, X., Zhu, Y., Zhang, Z., 2015. A comparative study of environmental performance between prefabricated and traditional residential buildings in China. J. Clean. Prod. 109, 131–143. https://doi.org/10.1016/j.jclepro.2015.04.120.

Chelouah, R., Siarry, P., 2000. Continuous genetic algorithm designed for the global optimization of multimodal functions. J. Heuristics 6, 191–213. https://doi.org/10.1023/A:1009626110229.

Cheng, J., Wang, J., Wu, X., Wang, S., 2019. An improved polynomial-based nonlinear variable importance measure and its application to degradation assessment for high-voltage transformer under imbalance data. Reliab. Eng. Syst. Saf. 185, 175–191. https://doi.org/10.1016/j.ress.2018.12.023.

Chou, J.S., Tsai, C.F., Pham, A.D., Lu, Y.H., 2014. Machine learning in concrete strength simulations: multi-nation data analytics. Construct. Build. Mater. 73, 771–780. https://doi.org/10.1016/j.conbuildmat.2014.09.054.

Chu, Y.-M., Shankaralingappa, B.M., Gireesha, B.J., Alzahrani, F., Khan, M.I., Khan, S.U., 2022. Combined impact of Cattaneo-Christov double diffusion and radiative heat flux on bio-convective flow of Maxwell liquid configured by a stretched nano-material surface. Appl. Math. Comput. 419, 126883. https://doi.org/10.1016/J.AMC.2021.126883.

Cooke, P., 2005. Regionally asymmetric knowledge capabilities and open innovation: exploring “Globalisation 2” - a new model of industry organisation. Res. Policy. 34, 1128–1149. https://doi.org/10.1016/j.respol.2004.12.005.

Corotis, R.B., 1988. Probability and statistics in civil engineering. Struct. Saf. 5, 321. https://doi.org/10.1016/0167-4730(88)90033-1.

Debasish Saha Roy, P., Kumar Tiwari, P., Preetam Debasish Saha Roy, B., 2019. Knowledge discovery and predictive accuracy comparison of different classification algorithms for mould level fluctuation phenomenon in thin slab caster. J. Intell. Manuf. 30, 241–254. https://doi.org/10.1007/s10845-016-1242-x.

Despotovic, M., Nedic, V., Despotovic, D., Cvetanovic, S., 2016. Evaluation of empirical models for predicting monthly mean horizontal diffuse solar radiation. Renew. Sustain. Energy Rev. 56, 246–260. https://doi.org/10.1016/j.rser.2015.11.058.

di Laurea di Edoardo Giovanni Colombo Matricola, T., Zanero Lorenzo Cavallaro Correlatori Federico Maggi Relatore, S., di Milano Antonio Lioy Relatore, P., di Torino, P., 2014. Laurea magistrale in ingegneria informatica detection and characterization of automatically-generated malicious domains CERBERUS. https://www.politesi.polimi.it/handle/10589/92341. (Accessed 30 March 2021).

Eijgelaar, E., Thaper, C., Peeters, P., 2010. Antarctic cruise tourism: the paradoxes of ambassadorship, “last chance tourism” and greenhouse gas emissions. J. Sustain. Tourism 18, 337–354. https://doi.org/10.1080/09669581003653534.

Erdal, H.I., 2013. Two-level and hybrid ensembles of decision trees for high performance concrete compressive strength prediction. Eng. Appl. Artif. Intell. 26, 1689–1697. https://doi.org/10.1016/j.engappai.2013.03.014.

Fakhrian, S., Behbahani, H., Mashhadi, S., 2020. Journal of soft computing in civil engineering predicting post-fire behavior of green geopolymer mortar containing recycled concrete aggregate via GEP approach ARTICLE INFO ABSTRACT. J. Soft Comput. Civ. Eng. 4, 22–45. https://doi.org/10.22115/SCCE.2020.220919.1182.

Faradonbeh, R.S., Hasanipanah, M., Amnieh, H.B., Armaghani, D.J., Monjezi, M., 2018. Development of GP and GEP models to estimate an environmental issue induced by blasting operation. Environ. Monit. Assess. 190, 1–15. https://doi.org/10.1007/s10661-018-6719-y.

Farooq, F., Amin, M.N., Khan, K., Sadiq, M.R., Javed, M.F., Aslam, F., Alyousef, R., 2020. A comparative study of random forest and genetic engineering programming for the prediction of compressive strength of high strength concrete (HSC). Appl. Sci. 10, 1–18. https://doi.org/10.3390/app10207330.

Farooq, F., Ahmed, W., Akbar, A., Aslam, F., Alyousef, R., 2021. Predictive modeling for sustainable high-performance concrete from industrial wastes: a comparison and optimization of models using ensemble learners. J. Clean. Prod. 292, 126032. https://doi.org/10.1016/j.jclepro.2021.126032.

Ferreira, C., 2001. Gene expression programming: a new adaptive algorithm for solving problems. http://arxiv.org/abs/cs/0102027. (Accessed 30 March 2021).

Fidan, S., Oktay, H., Polat, S., Ozturk, S., 2019. An artificial neural network model to predict the thermal properties of concrete using different neurons and activation functions. Adv. Mater. Sci. Eng. 2019 https://doi.org/10.1155/2019/3831813.

Fouilloy, A., Voyant, C., Notton, G., Motte, F., Paoli, C., Nivet, M.L., Guillot, E., Duchaud, J.L., 2018. Solar irradiation prediction with machine learning: forecasting models selection method depending on weather variability. Energy 165, 620–629. https://doi.org/10.1016/j.energy.2018.09.116.

Gandomi, A.H., Alavi, A.H., Mirzahosseini, M.R., Nejad, F.M., 2011. Nonlinear genetic-based models for prediction of flow number of asphalt mixtures. J. Mater. Civ. Eng. 23, 248–263. https://doi.org/10.1061/(asce)mt.1943-5533.0000154.

Gandomi, A.H., Faramarzifar, A., Rezaee, P.G., Asghari, A., Talatahari, S., 2015. New design equations for elastic modulus of concrete using multi expression programming. J. Civ. Eng. Manag. 21, 761–774. https://doi.org/10.3846/13923730.2014.893910.

Giorgio, V., Dovìa, D., Friedler, F., Huisingh, D., Klemeš, J.J., 2009. Cleaner energy for sustainable future. J. Clean. Prod. 1–7. https://doi.org/10.1016/j.jclepro.2009.02.001.

Golafshani, E.M., Ashour, A., 2016. Prediction of self-compacting concrete elastic modulus using two symbolic regression techniques. Autom. ConStruct. 64, 7–19. https://doi.org/10.1016/j.autcon.2015.12.026.

Golbraikh, A., Tropsha, A., 2002. Beware of q2. In: J. Mol. Graph. Model. Elsevier, pp. 269–276. https://doi.org/10.1016/S1093-3263(01)00123-1.

Gong, H., Sun, Y., Shu, X., Huang, B., 2018. Use of random forests regression for predicting IRI of asphalt pavements. Construct. Build. Mater. 189, 890–897. https://doi.org/10.1016/j.conbuildmat.2018.09.017.

Güllü, H., 2017. A novel approach to prediction of rheological characteristics of jet grout cement mixtures via genetic expression programming. Neural Comput. Appl. 28, 407–420. https://doi.org/10.1007/s00521-016-2360-2.

hai He, Z., nan Zhu, H., yuan Zhang, M., yan Shi, J., gui Du, S., Liu, B., 2021a. Autogenous shrinkage and nano-mechanical properties of UHPC containing waste brick powder derived from construction and demolition waste. Construct. Build. Mater. 306, 124869. https://doi.org/10.1016/J.CONBUILDMAT.2021.124869.

hai He, Z., Yang, Y., Yuan, Q., yan Shi, J., ju Liu, B., feng Liang, C., gui Du, S., 2021b. Recycling hazardous water treatment sludge in cement-based construction materials: mechanical properties, drying shrinkage, and nano-scale characteristics. J. Clean. Prod. 290, 125832. https://doi.org/10.1016/J.JCLEPRO.2021.125832.

Han, Q., Gui, C., Xu, J., Lacidogna, G., 2019. A generalized method to predict the compressive strength of high-performance concrete by improved random forest algorithm. Construct. Build. Mater. 226, 734–742. https://doi.org/10.1016/j.conbuildmat.2019.07.315.

Haque, M., Ray, S., Mita, A.F., Bhattacharjee, S., Bin Shams, M.J., 2021. Prediction and optimization of the fresh and hardened properties of concrete containing rice husk ash and glass fiber using response surface methodology. Case Stud. Constr. Mater. 14, e00505 https://doi.org/10.1016/J.CSCM.2021.E00505.

Hashmi, M.Z., Shamseldin, A.Y., Melville, B.W., 2011. Statistical downscaling of watershed precipitation using Gene Expression Programming (GEP). Environ. Model. Software 26, 1639–1646. https://doi.org/10.1016/j.envsoft.2011.07.007.

He, Z., Zhu, H., Shi, J., Li, J., Yuan, Q., Ma, C., 2022. Multi-scale characteristics of magnesium potassium phosphate cement modified by metakaolin. Ceram. Int. https://doi.org/10.1016/J.CERAMINT.2022.01.112.

Hornik, K., Leisch, F., Zeileis, A., Furlanello, C., Neteler, M., Merler, S., Menegon, S., Fontanari, S., Donini, A., Rizzoli, A., Chemini, C.. GIS and the random forest predictor: integration in R for tick-borne disease risk assessment. n.d. http://www.ci.tuwien.ac.at/Conferences/DSC-2003/. (Accessed 30 March 2021).

Ihedioha, J.N., Ukoha, P.O., Ekere, N.R., 2017. Ecological and human health risk assessment of heavy metal contamination in soil of a municipal solid waste dump in Uyo, Nigeria. Environ. Geochem. Health 39, 497–515. https://doi.org/10.1007/s10653-016-9830-4.

Jalal, F.E., Xu, Y., Iqbal, M., Javed, M.F., Jamhiri, B., 2021. Predictive modeling of swell-strength of expansive soils using artificial intelligence approaches: ANN, ANFIS and GEP. J. Environ. Manag. 289, 112420. https://doi.org/10.1016/J.JENVMAN.2021.112420.

Javed, M.F., Farooq, F., Memon, S.A., Akbar, A., Khan, M.A., Aslam, F., Alyousef, R., Alabduljabbar, H., Ur Rehman, S.K., 2020. New prediction model for the ultimate axial capacity of concrete-filled steel tubes: an evolutionary approach. Crystals 10, 1–33. https://doi.org/10.3390/cryst10090741.

Kaveh, A., Bakhshpoori, T., Hamze-Ziabari, S.M., 2018. M5' and mars based prediction models for properties of selfcompacting concrete containing fly ash. Period. Polytech. Civ. Eng. 62, 281–294. https://doi.org/10.3311/PPci.10799.

Khan, M.A., Memon, S.A., Farooq, F., Javed, M.F., Aslam, F., Alyousef, R., 2021a. Compressive strength of fly-ash-based geopolymer concrete by gene expression programming and random forest. Adv. Civ. Eng. 2021 https://doi.org/10.1155/2021/6618407.

Khan, M.A., Zafar, A., Farooq, F., Javed, M.F., Alyousef, R., Alabduljabbar, H., Khan, M. I., 2021b. Geopolymer concrete compressive strength via artificial neural network, adaptive neuro fuzzy interface system, and gene expression programming with K-fold cross validation. Front. Mater. 8 https://doi.org/10.3389/fmats.2021.621163.

Kohavi, R., 1995. A study of cross-validation and bootstrap for accuracy estimation and model selection. Int. Jt. Conf. Artif. Intell.

Liu, B., Shi, J., Zhou, F., Shen, S., Ding, Y., Qin, J., 2020. Effects of steam curing regimes on the capillary water absorption of concrete: prediction using multivariable regression models. Construct. Build. Mater. 256, 119426. https://doi.org/10.1016/J.CONBUILDMAT.2020.119426.

Liu, B., Qin, J., Shi, J., Jiang, J., Wu, X., He, Z., 2021. New perspectives on utilization of CO2 sequestration technologies in cement-based materials. Construct. Build. Mater. 272, 121660. https://doi.org/10.1016/J.CONBUILDMAT.2020.121660.

Lu, Z., Lu, C., Leung, C.K.Y., Li, Z., 2019a. Graphene oxide modified Strain Hardening Cementitious Composites with enhanced mechanical and thermal properties by incorporating ultra-fine phase change materials. Cement Concr. Compos. 98, 83–94. https://doi.org/10.1016/J.CEMCONCOMP.2019.02.010.

Lu, X., Zhou, W., Ding, X., Shi, X., Luan, B., Li, M., 2019b. Ensemble learning regression for estimating unconfined compressive strength of cemented paste backfill. IEEE Access 7, 72125–72133. https://doi.org/10.1109/ACCESS.2019.2918177.

Lv, Z., Jiang, A., Jin, J., Lv, X., 2021. Multifractal analysis and compressive strength prediction for concrete through acoustic emission parameters. Adv. Civ. Eng. 2021 https://doi.org/10.1155/2021/6683878.

Mahdinia, S., Eskandari-Naddaf, H., Shadnia, R., 2019. Effect of cement strength class on the prediction of compressive strength of cement mortar using GEP method. Construct. Build. Mater. 198, 27–41. https://doi.org/10.1016/j.conbuildmat.2018.11.265.

Mikulčić, H., Klemeš, J.J., Vujanović, M., Urbaniec, K., Duić, N., 2016. Reducing greenhouse gasses emissions by fostering the deployment of alternative raw materials and energy sources in the cleaner cement manufacturing process. J. Clean. Prod. 136, 119–132. https://doi.org/10.1016/j.jclepro.2016.04.145.

Napoli, A., Realfonzo, R., 2020. Compressive strength of concrete confined with fabric reinforced cementitious matrix (FRCM): analytical models. Compos. Part C Open Access 2, 100032. https://doi.org/10.1016/j.jcomc.2020.100032.

Nguyen, T., Kashani, A., Ngo, T., Bordas, S., 2019. Deep neural network with high-order neuron for the prediction of foamed concrete strength. Comput. Civ. Infrastruct. Eng. 34, 316–332. https://doi.org/10.1111/MICE.12422.

Nguyen, K.T., Nguyen, Q.D., Le, T.A., Shin, J., Lee, K., 2020. Analyzing the compressive strength of green fly ash based geopolymer concrete using experiment and machine learning approaches. Construct. Build. Mater. 247, 118581. https://doi.org/10.1016/J.CONBUILDMAT.2020.118581.

Nilsen, V., Pham, L.T., Hibbard, M., Klager, A., Cramer, S.M., Morgan, D., 2019. Prediction of concrete coefficient of thermal expansion and other properties using machine learning. Construct. Build. Mater. 220, 587–595. https://doi.org/10.1016/j.conbuildmat.2019.05.006.

Ozcan, G., Kocak, Y., Gulbandilar, E., 2017. Estimation of compressive strength of BFS and WTRP blended cement mortars with machine learning models. Comput. Concr. 19, 275–282. https://doi.org/10.12989/cac.2017.19.3.275.

Paris, J.M., Roessler, J.G., Ferraro, C.C., Deford, H.D., Townsend, T.G., 2016. A review of waste products utilized as supplements to Portland cement in concrete. J. Clean. Prod. 121, 1–18. https://doi.org/10.1016/j.jclepro.2016.02.013.

Peng, Y.Z., Yuan, C.A., Qin, X., Huang, J.T., Shi, Y.B., 2014. An improved Gene Expression Programming approach for symbolic regression problems. Neurocomputing 137, 293–301. https://doi.org/10.1016/j.neucom.2013.05.062.

Poli, R., 2001. Evolution of Graph-like Programs with Parallel Distributed Genetic Programming Improving Group Decision Making with Collaborative Brain-Computer Interfaces View Project Evolutionary Computation for Image Processing and Analysis View Project Parallel Distributed Genetic Programming. https://www.researchgate.net/publication/2416404. (Accessed 30 March 2021).

Prasad, B.K.R., Eskandari, H., Reddy, B.V.V., 2009. Prediction of compressive strength of SCC and HPC with high volume fly ash using ANN. Construct. Build. Mater. 23, 117–128. https://doi.org/10.1016/j.conbuildmat.2008.01.014.

Rahla, K.M., Mateus, R., Bragança, L., 2019. Comparative sustainability assessment of binary blended concretes using supplementary cementitious materials (SCMs) and ordinary Portland cement (OPC). J. Clean. Prod. 220, 445–459. https://doi.org/10.1016/J.JCLEPRO.2019.02.010.

Rajaee, T., Khani, S., Ravansalar, M., 2020. Artificial intelligence-based single and hybrid models for prediction of water quality in rivers: a review. Chemometr. Intell. Lab. Syst. 200, 103978. https://doi.org/10.1016/j.chemolab.2020.103978.

Ramezanianpour, A.A., Mahdikhani, M., Ahmadibeni, G., 2009. The effect of rice husk ash on mechanical properties and durability of sustainable concretes. Int. J. Civ. Eng. 7, 83–91.

Rao, G.A., 2001. Role of water-binder ratio on the strength development in mortars incorporated with silica fume. Cement Concr. Res. 31, 443–447. https://doi.org/10.1016/S0008-8846(00)00500-7.

Rehan, R., Nehdi, M., 2005. Carbon dioxide emissions and climate change: policy implications for the cement industry. Environ. Sci. Pol. 8, 105–114. https://doi.org/10.1016/j.envsci.2004.12.006.

Rokach, L., Maimon, O., 2014. Data Mining with Decision Trees. WORLD SCIENTIFIC. https://doi.org/10.1142/9097.

Roy, P.P., Roy, K., 2008. On some aspects of variable selection for partial least squares regression models. QSAR Comb. Sci. 27, 302–313. https://doi.org/10.1002/qsar.200710043.

Saha, P., Debnath, P., Thomas, P., 2020. Prediction of fresh and hardened properties of self-compacting concrete using support vector regression approach. Neural Comput. Appl. 32, 7995–8010. https://doi.org/10.1007/s00521-019-04267-w.

Saloma, A. Nasution, Imran, I., Abdullah, M., 2015. Improvement of concrete durability by nanomaterials. In: Procedia Eng. Elsevier Ltd, pp. 608–612. https://doi.org/10.1016/j.proeng.2015.11.078.

Saridemir, M., 2010. Genetic programming approach for prediction of compressive strength of concretes containing rice husk ash. Construct. Build. Mater. 24, 1911–1919. https://doi.org/10.1016/J.CONBUILDMAT.2010.04.011.

Sathyan, D., Anand, K.B., Prakash, A.J., Premjith, B., 2018. Modeling the fresh and hardened stage properties of self-compacting concrete using random kitchen sink algorithm. Int. J. Concr. Struct. Mater. 12, 1–10. https://doi.org/10.1186/s40069-018-0246-7.

Saud, S., Jamil, B., Upadhyay, Y., Irshad, K., 2020. Performance improvement of empirical models for estimation of global solar radiation in India: a k-fold cross-validation approach. Sustain. Energy Technol. Assessments 40. https://doi.org/10.1016/j.seta.2020.100768.

Schorcht, F., Ioanna, K., Bianca Maria, S., Serge, R., Luis, D.S., 2013. BAT Document for the Production of Cement. https://doi.org/10.2788/12850.

Selvaraj, S., Sivaraman, S., 2019. Prediction model for optimized self-compacting concrete with fly ash using response surface method based on fuzzy classification. Neural Comput. Appl. 31, 1365–1373. https://doi.org/10.1007/s00521-018-3575-1.

Severcan, M.H., 2012. Prediction of splitting tensile strength from the compressive strength of concrete using GEP. Neural Comput. Appl. 21, 1937–1945. https://doi.org/10.1007/s00521-011-0597-3.

Shahmansouri, A.A., Akbarzadeh Bengar, H., Ghanbari, S., 2020. Compressive strength prediction of eco-efficient GGBS-based geopolymer concrete using GEP method. J. Build. Eng. 31, 101326. https://doi.org/10.1016/j.jobe.2020.101326.

Shi, J., Liu, B., He, Z., Liu, Y., Jiang, J., Xiong, T., Shi, J., 2021. A green ultra-lightweight chemically foamed concrete for building exterior: a feasibility study. J. Clean. Prod. 288, 125085. https://doi.org/10.1016/J.JCLEPRO.2020.125085.

Siddique, R., Aggarwal, P., Aggarwal, Y., 2011. Prediction of compressive strength of self-compacting concrete containing bottom ash using artificial neural networks. Adv. Eng. Software 42, 780–786. https://doi.org/10.1016/j.advengsoft.2011.05.016.

Sivakami, K.. Mining big data: breast cancer prediction using DT-SVM hybrid model. n.d. www.ijseas.com. (Accessed 30 March 2021).

Supino, S., Malandrino, O., Testa, M., Sica, D., 2016. Sustainability in the EU cement industry: the Italian and German experiences. J. Clean. Prod. 112, 430–442. https://doi.org/10.1016/J.JCLEPRO.2015.09.022.

Tam, V.W.Y., Tam, C.M., 2006. A review on the viable technology for construction waste recycling. Resour. Conserv. Recycl. 47, 209–221. https://doi.org/10.1016/j.resconrec.2005.12.002.

Tang, P., Chen, W., Xuan, D., Zuo, Y., Poon, C.S., 2020. Investigation of cementitious properties of different constituents in municipal solid waste incineration bottom ash as supplementary cementitious materials. J. Clean. Prod. 258, 120675. https://doi.org/10.1016/j.jclepro.2020.120675.

Tin Lee, C., Hashim, H., Siong Ho, C., Van Fan, Y., Jaromír Klemeš, J., Johor Bahru, U., Bahru, J., 2016. Sustaining the low-carbon emission development in Asia and beyond: sustainable energy, water, transportation and low-carbon emission technology. http://www.elsevier.com/open-access/userlicense/1.0/. (Accessed 4 March 2022).

Vakhshouri, B., Nejadi, S., 2018. Prediction of compressive strength of self-compacting concrete by ANFIS models. Neurocomputing 280, 13–22. https://doi.org/10.1016/j.neucom.2017.09.099.

Van Dao, D., Ly, H.-B., Vu, H.-L.T., Le, T.-T., Pham, B.T., 2020. Investigation and optimization of the C-ANN structure in predicting the compressive strength of foamed concrete. Materials 13, 1072. https://doi.org/10.3390/ma13051072.

Xiao, J., 2018. Recycled aggregate concrete. In: Springer Tracts Civ. Eng. Springer, pp. 65–98. https://doi.org/10.1007/978-3-662-53987-3_4.

Xu, M., Watanachaturaporn, P., Varshney, P.K., Arora, M.K., 2005. Decision tree regression for soft classification of remote sensing data. Remote Sens. Environ. 97, 322–336. https://doi.org/10.1016/j.rse.2005.05.008.

Yaşar, E., Erdogan, Y., Kiliç, A., 2004. Effect of limestone aggregate type and water-cement ratio on concrete strength. Mater. Lett. 58, 772–777. https://doi.org/10.1016/j.matlet.2003.06.004.

Zha, T.H., Castillo, O., Jahanshahi, H., Yusuf, A., Alassafi, M.O., Alsaadi, F.E., Chu, Y.M., 2021. A fuzzy-based strategy to suppress the novel coronavirus (2019-NCOV) massive outbreak. Appl. Comput. Math. 160–176.

Zhang, J., Ma, G., Huang, Y., sun, J., Aslani, F., Nener, B., 2019. Modelling uniaxial compressive strength of lightweight self-compacting concrete using random forest regression. Construct. Build. Mater. 210, 713–719. https://doi.org/10.1016/j.conbuildmat.2019.03.189.

Zhao, T.-H., Wang, M.-K., Hai, G.-J., Chu, Y.-M., 2021a. Landen inequalities for Gaussian hypergeometric function. Rev. La Real Acad. Ciencias Exactas, Físicas y Nat. Ser. A. Matemáticas 116, 1–23. https://doi.org/10.1007/S13398-021-01197-Y, 2021 1161.

Zhao, T.H., Khan, M.I., Chu, Y.M., 2021b. Artificial neural networking (ANN) analysis for heat and entropy generation in flow of non-Newtonian fluid between two rotating disks. Math. Methods Appl. Sci. https://doi.org/10.1002/MMA.7310.